

LEVEL II

(12) SC

AD A061929

NOSC

NOSC TR 265

Z

Technical Report 265

MULTIPLE COHERENCE AS A DETECTION STATISTIC

RD Trueblood, DL Alspach

1 July 1978

Research and Development Report: January - April 1978

Prepared for
Advanced Research Projects Agency
Naval Electronics Systems Command

DDC FILE COPY

DDC
RECEIVED
DEC 8 1978
RECEIVED

APPROVED FOR PUBLIC RELEASE; DISTRIBUTION UNLIMITED

NAVAL OCEAN SYSTEMS CENTER
SAN DIEGO, CALIFORNIA 92152

72 06 011



NAVAL OCEAN SYSTEMS CENTER, SAN DIEGO, CA 92152

AN ACTIVITY OF THE NAVAL MATERIAL COMMAND
RR GAVAZZI, CAPT, USN **HL BLOOD**

Commander

Technical Director

ADMINISTRATIVE INFORMATION

The work in the report was sponsored by the Advanced Research Projects Agency under ARPA order 3074, program element 62702E, and the Naval Electronic Systems Command under program element 62711N, project number XF11-121-60Z. Work was performed from January through April 1976. The work was done in part under contract N00123-76-C-0505 with ORINCON Corporation. D. L. Alspach, ORINCON Corp., is a co-author of this report.

Released by
D.A. HANNA, Head
Signal Processing and
Display Division

Under authority of
H.A. SCHENCK, Head
Undersea Surveillance
Department

The views and conclusions contained in this document are those of the authors and should not be interpreted as necessarily representing the official policies, either expressed or implied, of the Defense Advanced Research Projects Agency or the U.S. Government.

UNCLASSIFIED

SECURITY CLASSIFICATION OF THIS PAGE (When Data Entered)

REPORT DOCUMENTATION PAGE		READ INSTRUCTIONS BEFORE COMPLETING FORM	
1. REPORT NUMBER NOSC TR 265	2. GOVT ACCESSION NO. TR-265	3. RECIPIENT'S CATALOG NUMBER	
4. TITLE (and Subtitle) MULTIPLE COHERENCE AS A DETECTION STATISTIC		5. TYPE OF REPORT & PERIOD COVERED Research and Development January through April 1976	6. PERFORMING ORG. REPORT NUMBER
7. AUTHOR(s) R. D. Trueblood / D. L. Alspach		8. CONTRACT OR GRANT NUMBER(s) N00123-76-C-0505, ARPA Order-3074	
9. PERFORMING ORGANIZATION NAME AND ADDRESS Naval Ocean Systems Center San Diego, California 92132		10. PROGRAM ELEMENT PROJECT, TASK AREA & WORK UNIT NUMBERS NOSC 62711N, XF11-121-60Z	
11. CONTROLLING OFFICE NAME AND ADDRESS Advanced Research Projects Agency Naval Electronics Systems Command		12. REPORT DATE July 1978	13. NUMBER OF PAGES 98
14. MONITORING AGENCY NAME & ADDRESS (if different from Controlling Office) F44422		15. SECURITY CLASS. (of this report) Unclassified	
16. DISTRIBUTION STATEMENT (of this Report) Approved for public release, distribution unlimited. XF4442260Z 62 p.			
17. DISTRIBUTION STATEMENT (of the abstract entered in DTIC-20, if different from Report) Technical rept. Jan-Apr 78			
18. SUPPLEMENTARY NOTES			
19. KEY WORDS (Continue on reverse side if necessary and identify by block number) Multiple coherence Detection statistic Signal processing			
20. ABSTRACT (Continue on reverse side if necessary and identify by block number) In this report, a sample statistic for the pairwise and multiple magnitude-squared coherence is investigated. The concept of coherence and its relationship to signal to noise ratios is discussed. The distribution of a sample statistic conditioned on the true coherence of the signals is given and plotted for various values of true coherence, degrees of freedom and number of time series. These distributions are used to produce receiver			

UNCLASSIFIED

SECURITY CLASSIFICATION OF THIS PAGE (When Data Entered)

392 776

elt

UNCLASSIFIED

SECURITY CLASSIFICATION OF THIS PAGE (When Data Entered)

20. (Continued)

operating characteristic curves and plots of probability of detection versus true coherence for fixed values of false alarm.

UNCLASSIFIED

SECURITY CLASSIFICATION OF THIS PAGE(When Data Entered)

CONTENTS

SECTION 1.0 INTRODUCTION AND SUMMARY . . .	page 1
SECTION 2.0 CROSS-POWER SPECTRAL DENSITY MATRIX AND MULTIPLE COHERENCE . . .	5
SECTION 3.0 PAIRWISE COHERENCE AND SIGNAL-TO-NOISE RATIOS . . .	9
SECTION 4.0 MULTIPLE COHERENCE AND SIGNAL-TO-NOISE RATIOS . . .	13
SECTION 5.0 A SAMPLE STATISTIC FOR MULTIPLE COHERENCE . . .	21
SECTION 6.0 DISTRIBUTION OF SAMPLE STATISTICS . . .	23
SECTION 7.0 REFERENCES . . .	61

SECTION 1.0	
ETER	GROUP NUMBER
QUC	QUC NUMBER
UNCLASSIFIED	
JUSTIFICATION	
BY	DISTRIBUTION AUTHORITY CODE
RISE	ARAB. ALL. M. SPECIAL
A	

SECTION 1.0 INTRODUCTION AND SUMMARY

A problem of interest in many different disciplines is that of determining if there is a measurable relationship (physical causality) between two or more time series. In addition, one would often like to obtain a quantitative meaningful measure of the degree of that relationship. This report describes one possible measure of such a relationship, the coherence.

The most common measure of such a relationship is the pairwise or multiple correlation coefficient. The nature of the correlation coefficient is well documented and will not be discussed here other than to note that it is not a function of frequency and may be affected by linear transformations of either of the time series.

The coherence function (magnitude-squared multiple or pairwise coherence function) is defined as a frequency-dependent quantity that ranges between zero and one (section 2 and references 2-9 and 16). This coherence function is zero if the Gaussian, ergodic time series are independent (uncorrelated) and equal to one at any frequency where there is a linear transformation between the one or more input time series and the output or reference time series.

The situation of interest is shown in figure 1.1 where v_i indicates the noise contaminating the signal $u(i)$ in the i^{th} channel. In general, each transmission channel is composed of linear and nonlinear parts (figure 1.2). The sum of the output of the nonlinear system (usually a small part of the total transmission), the measurement noise, and the background noise is grouped into the effective noise term $v_i(t)$ (figure 1.3).

We are interested in detecting the presence of a common signal $u(t)$ in two or more channels. The input-output relationship indicated in figure 1.3 can be written as

$$\begin{bmatrix} x_1(t) \\ x_2(t) \\ \vdots \\ x_M(t) \end{bmatrix} = \int_{-\infty}^{\infty} \begin{bmatrix} g_1(\tau) \\ g_2(\tau) \\ \vdots \\ g_M(\tau) \end{bmatrix} u(t - \tau) d\tau + \begin{bmatrix} v_1(t) \\ v_2(t) \\ \vdots \\ v_M(t) \end{bmatrix} \quad (1.1a)$$

or more concisely as

$$\underline{x}(t) = \int_{-\infty}^{\infty} \underline{g}(\tau) u(t - \tau) d\tau + \underline{v}(t). \quad (1.1b)$$

Note that because of physical causality requirements, $g(\tau)$ is zero for all τ less than zero. In fact, it will be zero for all τ less than some positive time which is the time it takes the signal to travel from the source to the sensor.

The true value of the coherence between time series is generally an unknown quantity. In fact, any measure of the relationship between two or more time series generally must be based on time traces of those series. The functional relationship between the time series and the measure or estimate of coherence is called a sample statistic for coherence (section 5). The assumption that any one infinite length sample of each series will be enough to allow us to estimate the coherence is made implicitly. Thus for this report all time series are assumed to be stationary and ergodic. Unfortunately, in practice, one is given only a finite amount of data from each of the time series. In this case the sample statistic is a random variable distributed about the "true magnitude-squared coherence." The density function for the sample statistic defined in section 5 is described and plotted in section 6 of this report.

Based on the density functions of section 6, receiver operation characteristic (ROC) curves are also given in section 6. These curves define the probability of detection versus probability of false alarm for a signal of a given true coherence. Also shown in this section are curves of probability of detection versus true coherence for fixed levels of probability of false alarm.

In sections 3 and 4 the relationship between input signal to noise levels and true coherence for the two-channel and multichannel cases are discussed.

For a general discussion of the concept of coherence, the reader is directed to reference 5 and sections 2 and 3 of this report. For a detailed derivation of the distribution of the pairwise and multiple coherence function discussed in section 6 of this report, the reader is referred to reference 7. The densities and derived performance curves in section 6 are particularly difficult to obtain for low coherence and high values of N (number of samples of the time series), and based on the authors' knowledge are not available elsewhere in the literature.

Thus the results in this report describe one approach to obtaining a quantitative measure of the degree of relationship between M -time series. This report precisely defines the detection performance possible when a common signal exists in M -series in the form of receiver operating curves. The precise performance expected is also given in terms of probability of detection versus true coherence for a number of different probabilities of false alarm and for various numbers of time series M .

Calculation of the multiple coherence between various output signals, $x_1(t)$, $x_2(t)$, ..., $x_M(t)$ allows the simultaneous use of data from M sensors and should have several advantages over using simply pairwise coherence. First, it should allow improved detection performance, i.e., it should be possible under certain circumstances to detect the presence of a mutual signal in all M channels when it is not quite possible to make such a detection using any two pairs. Secondly, it provides a natural way to include additional sensor information. It does not require the addition of a large number of new test statistics each time a new sensor is introduced, a situation which may occur when all possible pairs are separately inspected. Thirdly, detection can occur using this one statistic even when the signal-to-noise ratio varies on the individual channels. This would allow signal-to-noise in one channel to go down while another one came up, without reducing the detection performance and without changing to a new statistic.

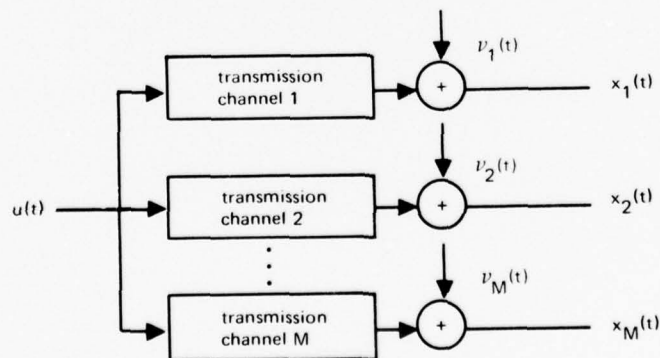


Figure 1.1. One input-or-output system.

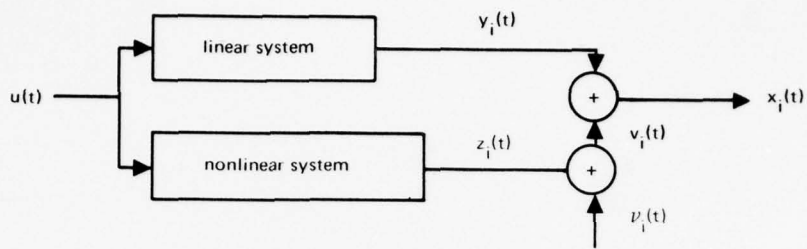


Figure 1.2. Linear and nonlinear parts of a single channel.

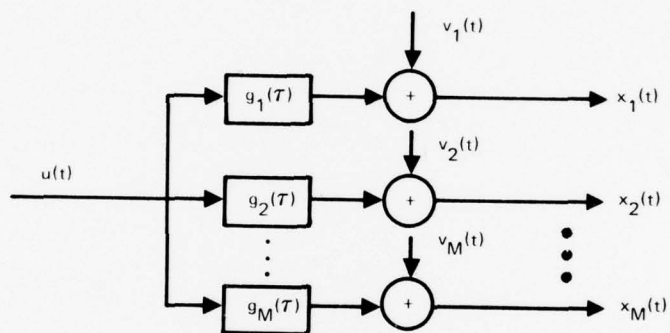


Figure 1.3. Effective noise with M linear transmission channels.

SECTION 2.0 CROSS-POWER SPECTRAL DENSITY MATRIX AND MULTIPLE COHERENCE

Multiple coherence can be most easily defined in terms of the cross spectral density matrix $S_{\underline{X}\underline{X}}(\omega)$, where

$$S_{\underline{X}\underline{X}}(\omega) = \begin{bmatrix} S_{11}(\omega) & S_{12}(\omega) & \dots & S_{1M}(\omega) \\ S_{21}(\omega) & S_{22}(\omega) & \dots & S_{2M}(\omega) \\ \dots & \dots & \dots & \dots \\ S_{M1}(\omega) & S_{M2}(\omega) & \dots & S_{MM}(\omega) \end{bmatrix}. \quad (2.1)$$

If i is not equal to j , $S_{ij}(\omega)$ represents the crosspower spectral density between the signals $x_i(t)$ and $x_j(t)$:

$$S_{ij}(\omega) \triangleq S_{x_i x_j}(\omega) = S_{ji}^*(\omega). \quad (2.2a)$$

As indicated by equation 2.2, this crosspower spectral density is generally complex for real signals $[x_i(t)$ and $x_j(t)]$. If i does equal j , the element $S_{ii}(\omega)$ represents the autopower spectral density of the i th signal $x_i(t)$ which is real and positive:

$$S_{ii}(\omega) = S_{x_i}(\omega). \quad (2.2b)$$

The crosspower spectral density matrix is of course equivalent to the crosscorrelation matrix. Either of these together with the means of the M jointly Gaussian stationary processes, $x_1(t)$, $x_2(t)$, \dots , $x_M(t)$, completely specifies the joint distribution function of these processes.

Given M finite length time traces, there are well known techniques for obtaining "sample estimates" of the cross- and autopower spectral elements. These estimates are used to obtain sample estimates for the multiple coherence between the various time series.

The sample estimate for the crosspower spectral density matrix is a function of the basic data $x_1(t)$, $x_2(t)$, \dots , $x_M(t)$ over some finite time record. It does not require knowledge of any of the characteristics of the transmission channels or of the signal-to-noise ratios of the received signals. The meaning of multiple coherence will be discussed in terms of these quantities in later sections in an attempt to illuminate the subject. Here, however, we will define multiple coherence simply in terms of the crosspower spectral density matrix and its elements.

The multiple coherence between $x_j(t)$ and $x_1(t), x_2(t), \dots, x_{j-1}(t), x_{j+1}(t), \dots, x_M(t)$ is defined by (reference 5)

$$|\gamma_{j:1,2 \dots j-1, j+1, \dots, N}|^2 = 1 - 1/[S_{jj}(\omega)S^{jj}(\omega)], \quad (2.3)$$

where $S^{jj}(\omega)$ is the j th diagonal element of the inverse of the $S_{XX}(\omega)$ matrix:

$$S_{XX}^{-1}(\omega) = \begin{bmatrix} S^{11}(\omega) & S^{12}(\omega) & \dots & S^{1M}(\omega) \\ S^{21}(\omega) & S^{22}(\omega) & \dots & S^{2M}(\omega) \\ \vdots & \vdots & \ddots & \vdots \\ S^{M1}(\omega) & S^{M2}(\omega) & \dots & S^{MM}(\omega) \end{bmatrix}. \quad (2.4)$$

Again it can easily be seen that $S^{ii}(\omega)$ is real and that $S^{ij}(\omega)$ is equal to $S^{ji}(\omega)^*$. The multiple coherence of the j th sensor with respect to the other sensors represents the proportion of the variance (power) of sensor j that can be explained by a linear combination of the remaining sensors in a minimum mean square sense (reference 2).

By reducing this definition to the simple two-channel case we can write

$$S_{XX}^{-1}(\omega) = \frac{1}{S_{11}(\omega)S_{22}(\omega) - |S_{12}(\omega)|^2} \begin{bmatrix} S_{22}(\omega) - S_{12}(\omega) \\ -S_{12}^*(\omega) \ S_{11}(\omega) \end{bmatrix}, \quad (2.5)$$

so that

$$S^{11}(\omega) = S_{22}(\omega)/[S_{11}(\omega)S_{22}(\omega) - |S_{12}(\omega)|^2]. \quad (2.6)$$

This gives

$$\begin{aligned} |\gamma_{1:2}(\omega)|^2 &= 1 - 1/[S_{11}(\omega)S^{11}(\omega)] \\ &= 1 - [S_{11}(\omega)S_{22}(\omega) - |S_{12}(\omega)|^2]/S_{11}(\omega)S_{22}(\omega) \\ &= |S_{12}(\omega)|^2/S_{11}(\omega)S_{22}(\omega), \end{aligned} \quad (2.7)$$

so that

$$|\gamma_{1:2}(\omega)|^2 = |\gamma_{2:1}(\omega)|^2 = |\gamma_{1,2}|^2 = \frac{|S_{12}(\omega)|^2}{S_{11}(\omega)S_{22}(\omega)}. \quad (2.8)$$

This is defined in section 3 as the mutual or pairwise coherence between channels one and two.

In the three-channel case it is easily seen (writing $S_{ij}(\omega)$ or S_{ij}) that $S^{11}(\omega)$ is given by

$$S^{11}(\omega) = [S_{22}S_{33} - |S_{23}|^2] / \text{DET}. \quad (2.9)$$

Here the determinant of the crosspower spectral matrix is given by

$$\begin{aligned} \text{DET} = & S_{11}S_{22}S_{33} - S_{11}|S_{23}|^2 - S_{33}|S_{21}|^2 - S_{22}|S_{31}|^2 \\ & + 2\text{Re}(S_{12}S_{23}S_{31}). \end{aligned} \quad (2.10)$$

Using this expression for the first diagonal element of the inverse of the crosspower spectral density matrix and the definition of the multiple coherence (equation 2.3) we find

$$\begin{aligned} |\gamma_{1:2,3}|^2 &= 1 - 1/(S_{11}(\omega)S^{11}(\omega)) \\ &= 1 - \frac{S_{11}S_{22}S_{33} - S_{11}|S_{23}|^2 - S_{33}|S_{21}|^2 - S_{22}|S_{31}|^2 + 2\text{Re}(S_{12}S_{23}S_{31})}{S_{11}S_{22}S_{33} - S_{11}|S_{23}|^2} \end{aligned} \quad (2.11)$$

or

$$|\gamma_{1:2,3}|^2 = \frac{S_{33}|S_{21}|^2 + S_{22}|S_{31}|^2 - 2\text{Re}(S_{12}S_{23}S_{31})}{S_{11}S_{22}S_{33} - S_{11}|S_{23}|^2}. \quad (2.12)$$

Using the fact that pairwise coherence is defined by

$$|\gamma_{i,j}|^2 = \frac{|S_{ij}|^2}{S_{ii}S_{jj}}, \quad (2.13)$$

we can write

$$|\gamma_{1:2,3}|^2 = \frac{|\gamma_{1,2}|^2 + |\gamma_{1,3}|^2 - 2\text{Re}(\gamma_{1,2}\gamma_{2,3}\gamma_{3,1})}{1 - |\gamma_{2,3}|^2}. \quad (2.14)$$

Note that if the crosspower spectral density of channels two and three is zero ($S_{23} = 0$), the coherence between these two channels is zero and the multiple coherence of channel one, given two and three, is

$$|\gamma_{1:2,3}|^2 = |\gamma_{1,2}|^2 + |\gamma_{1,3}|^2. \quad (2.15)$$

We know that $|\gamma_{1:2,3}|^2$ should be found between zero and one. However, this is not immediately clear from equation 2.14. In particular, when $|\gamma_{2,3}|^2$ goes to one the denominator in equation 2.14 goes to zero. This can be investigated by considering the case when $x_2(t)$ is generated as in figure 2.1:

$$x_2(t) = \int_{\alpha}^{\beta} x_3(\alpha) h_{23}(t - \alpha) d\alpha + \omega(t), \quad (2.16)$$

where $\omega(t)$ is a zero mean stochastic process uncorrelated with $x_1(t)$ and $x_3(t)$. In this system the auto- and crosspower spectral densities of channel two can be written as

$$\begin{aligned} S_{22}(\omega) &= |H_{23}(\omega)|^2 S_{33}(\omega) + W(\omega) \\ S_{12}(\omega) &= H_{23}(\omega) S_{13}(\omega) \\ S_{23}(\omega) &= H_{23}(\omega) S_{33}(\omega). \end{aligned} \quad (2.17)$$

Note that if $W(\omega)$ goes to zero the coherence $|\gamma_{2,3}|^2$ goes to one, which means that the denominator in equation 2.14 goes to zero. To investigate this, we can use these relationships (equation 2.17) in equation 2.14 to give

$$\begin{aligned} |\gamma_{1:2,3}|^2 &= \frac{S_{33} |H_{23}(\omega)|^2 |S_{13}|^2 + (|H_{23}(\omega)|^2 S_{33} + W) |S_{13}|^2 - 2 |S_{13}|^2 S_{33} |H_{23}(\omega)|^2}{S_{11} S_{33} [|H_{23}(\omega)|^2 S_{33} + W] - S_{11} |H_{23}(\omega)|^2 S_{33}^2} \\ &= \frac{|S_{13}|^2 W}{S_{33} S_{11} W} = \frac{|S_{13}|^2}{S_{11} S_{33}} = |\gamma_{1,3}|^2. \end{aligned} \quad (2.18)$$

Thus, if $x_2(t)$ can be generated by passing $x_3(t)$ through an arbitrary linear system and adding uncorrelated noise, then no new information is gained by processing the time series $x_2(t)$:

$$|\gamma_{1:2,3}|^2 = |\gamma_{1,3}|^2 \geq |\gamma_{1,2}|^2. \quad (2.19)$$

This result is independent of $W(\omega)$ and $|\gamma_{2,3}|^2$.

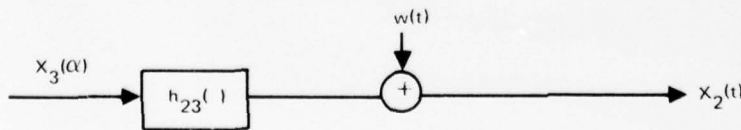


Figure 2.1. Generation of $x_2(t)$.

SECTION 3.0 PAIRWISE COHERENCE AND SIGNAL-TO-NOISE RATIOS

In reference 5 the ordinary magnitude-squared coherence of the signals $x_i(t)$, $x_j(t)$ is discussed and defined as

$$|Y_{i,j}|^2 = \frac{|S_{ij}(\omega)|^2}{S_{ii}(\omega) S_{jj}(\omega)} \quad (3.1)$$

From the definition of coherence, it is obvious that the coherence of channel i given j is the same as that of channel j given i .

If $x_1(t)$ and $x_2(t)$ are generated as indicated in figure 1.3, equation 1.1 can be written in the frequency domain by Fourier transform as

$$X_1(\omega) = G_1(\omega)U(\omega) + V_1(\omega) \quad (3.2)$$

$$X_2(\omega) = G_2(\omega)U(\omega) + V_2(\omega). \quad (3.3)$$

Again assuming the noise terms V_1 and V_2 are independent, the cross- and autopower spectral densities can be written as

$$S_{11}(\omega) = |G_1(\omega)|^2 S_u(\omega) + S_{V_1}(\omega) \quad (3.4)$$

$$S_{22}(\omega) = |G_2(\omega)|^2 S_u(\omega) + S_{V_2}(\omega) \quad (3.5)$$

$$|S_{12}(\omega)|^2 = |G_1(\omega)|^2 |G_2(\omega)|^2 S_u(\omega)^2. \quad (3.6)$$

Noting that $|G_1(\omega)|^2 S_u(\omega)$ and $|G_2(\omega)|^2 S_u(\omega)$ are the output signal power spectra at the receiver in channels one and two, we write the magnitude-squared coherence as

$$|Y_{1,2}|^2 = \frac{|G_1(\omega)|^2 |G_2(\omega)|^2 S_u(\omega)^2}{\left[|G_1(\omega)|^2 S_u(\omega) + S_{V_1}(\omega) \right] \left[|G_2(\omega)|^2 S_u(\omega) + S_{V_2}(\omega) \right]} \quad (3.7)$$

or

$$|Y_{1,2}|^2 = \frac{1}{\left[1 + S_{V_1}(\omega)/|G_1(\omega)|^2 S_u(\omega) \right] \left[1 + S_{V_2}(\omega)/|G_2(\omega)|^2 S_u(\omega) \right]} \quad (3.8)$$

Defining the signal-to-noise power in the j th channel as

$$(S/N)_j = \frac{|G_j(\omega)|^2 S_u(\omega)}{S_{v_j}(\omega)} \quad (3.9)$$

and the similar noise-to-signal ratio as

$$(N/S)_j = 1/(S/N)_j, \quad (3.10)$$

we can write

$$|\gamma_{1,2}|^2 = \frac{1}{[1 + (N/S)_1][1 + (N/S)_2]} = \frac{\left(\frac{S}{N}\right)_1}{\left[1 + \left(\frac{S}{N}\right)_1\right]} \cdot \frac{\left(\frac{S}{N}\right)_2}{\left[1 + \left(\frac{S}{N}\right)_2\right]}. \quad (3.11)$$

Certain general statements concerning this pairwise magnitude-squared coherence, or just "coherence," can now be made.

The coherence is bounded between zero and one:

$$0 \leq |\gamma_{1,2}|^2 \leq 1. \quad (3.12)$$

If the noise-to-signal power goes to infinity in either channel, the coherence will go to zero. This will happen if the signal power in that channel fades to zero. Also, the noise-to-signal power ratio in both channels must go to zero for the coherence to go to one.

An interesting and informative interpretation of the coherence between these two channels can be made in the following manner. Assume one of the channels is noise free:

$$S_{v_2}(\omega) = 0. \quad (3.13)$$

This channel then becomes the input signal. The coherence between channels one and two is now given by

$$|\gamma_{1,2}|^2 = \frac{|G_1(\omega)|^2 S_u(\omega)}{|G_1(\omega)|^2 S_u(\omega) + S_{v_1}(\omega)} = \frac{(S/N)_1}{1 + (S/N)_1} = \frac{S_1}{S_1 + N_1}. \quad (3.14)$$

This magnitude-squared coherence is the fraction of the power of the output $x_1(t)$ which comes from the signal input passed through a linear system.

Since the transmitted signal is generally not available, it is useful to look at this physical interpretation of coherence from a different point of view. Let us simply take signal $x_2(t)$ as our basic signal and calculate the coherence between $x_1(t)$ and our given signal $x_2(t)$. From equation 3.1, our definition, this will be the same result as if we took signal $x_1(t)$ as our "given" signal. Thus $U(\omega)$ in equation 3.2 is replaced by $X_2(\omega)$:

$$X_1(\omega) = H_{12}(\omega)X_2(\omega) + V_{e12}(\omega). \quad (3.15)$$

$H_{12}(\omega)$ is the effective linear transfer function between output $x_2(t)$ and output $x_1(t)$. $V_{e12}(t)$ is the effective noise on the transmission channel. It must be noted that $H_{12}(\omega)$ is no longer necessarily a causal system. Now the coherence between channels one and two can be written as in equation 3.14:

$$|Y_{1,2}(\omega)|^2 = \frac{|H_{12}(\omega)|^2 S_{22}(\omega)}{[|H_{12}(\omega)|^2 S_{22}(\omega) + S_{ve12}(\omega)]}. \quad (3.16)$$

This two-channel magnitude-squared coherence is the ratio of the power at output $x_1(t)$, which is caused by the "input $x_2(t)$," transmitted over the effective linear transmission channel $[H_{12}(\omega)]$ to the total power in output x_1 . Consideration of this effective linear transmission channel allows this physical interpretation of the coherence to be easily carried over to multiple coherence.

SECTION 4.0 MULTIPLE COHERENCE AND SIGNAL-TO-NOISE RATIOS

In the case of M channels, a relationship between the input signal-to-noise ratios and the multiple coherence, similar to the one in the last section for two channels, can be derived. The output power spectral density can again be written in terms of this input signal spectral density, the unknown channel transfer functions, and the effective channel noise as

$$S_{ii}(\omega) = |G_i(\omega)|^2 S_u(\omega) + S_{v_i}(\omega) \quad (4.1)$$

$$|S_{ij}(\omega)|^2 = |G_i(\omega)|^2 |G_j(\omega)|^2 S_u(\omega)^2, \quad i \neq j \quad (4.2)$$

It should be noted that $|G_i(\omega)|^2 S_u(\omega)$ is the signal power density in the output of the i th channel and $S_{v_i}(\omega)$ is the noise power spectral density in that channel. The general power spectral density function can then be written as

$$S_{XX}(\omega) = \begin{bmatrix} |G_1(\omega)|^2 S_u(\omega) + S_{v_1}(\omega) & G_1^*(\omega) G_2(\omega) S_u(\omega) & \dots & G_1^*(\omega) G_M(\omega) S_u(\omega) \\ G_2^*(\omega) G_1(\omega) S_u(\omega) & |G_2(\omega)|^2 S_u(\omega) + S_{v_2}(\omega) & \dots & G_2^*(\omega) G_M(\omega) S_u(\omega) \\ \cdot & \cdot & \cdot & \cdot \\ G_M^*(\omega) G_1(\omega) S_u(\omega) & G_M^*(\omega) G_2(\omega) S_u(\omega) & \dots & |G_M(\omega)|^2 S_u(\omega) + S_{v_M}(\omega) \end{bmatrix} \quad (4.3)$$

or in a more concise manner as

$$S_{XX}(\omega) = S_u(\omega) G^*(\omega) G^T(\omega) + D(\omega), \quad (4.4)$$

where

$$D(\omega) = \begin{bmatrix} S_{v_1}(\omega) & 0 & \dots & 0 \\ 0 & S_{v_2}(\omega) & \dots & 0 \\ \vdots & \vdots & \ddots & \vdots \\ 0 & 0 & \dots & S_{v_M}(\omega) \end{bmatrix} \quad (4.5)$$

and

$$G^T(\omega) = [G_1(\omega)G_2(\omega) \dots G_M(\omega)]. \quad (4.6)$$

The inverse required to calculate the multiple coherence from equation 2.3 can now be calculated by using the following matrix inversion lemma:

$$\left[A + X^* X^T \right]^{-1} = A^{-1} - A^{-1} X^* \left(1 + X^T A^{-1} X^* \right)^{-1} X^T A^{-1}. \quad (4.7)$$

Using this lemma, the inverse of the spectral density matrix can be written (assuming all required inverses exist) as

$$S_{\underline{X}\underline{X}}^{-1}(\omega) = D^{-1}(\omega) - S_u(\omega) D^{-1}(\omega) G^*(\omega) \left[1 + S_u(\omega) G^T(\omega) D^{-1}(\omega) G^*(\omega) \right]^{-1} G^T(\omega) D^{-1}(\omega). \quad (4.8)$$

The structure of this inverse can be seen more clearly by noting that

$$S_u(\omega) G^T(\omega) D^{-1}(\omega) G^*(\omega) = \frac{|G_1(\omega)|^2 S_u(\omega)}{S_{v_1}(\omega)} + \frac{|G_2(\omega)|^2 S_u(\omega)}{S_{v_2}(\omega)} + \dots + \frac{|G_M(\omega)|^2 S_u(\omega)}{S_{v_M}(\omega)}. \quad (4.9)$$

This term is the sum of all output signal-to-noise power ratios. Therefore, if, as in the two-channel case, we define

$$(S/N)_i = |G_i(\omega)|^2 S_u(\omega) / S_{v_i}(\omega) \quad (4.10)$$

the inverse of the bracketed term in equation 4.8 can be written as

$$\left[1 + S_u(\omega) G^T(\omega) D^{-1}(\omega) G^*(\omega) \right]^{-1} = 1 / \left[1 + \sum_{j=1}^M (S/N)_j \right]. \quad (4.11)$$

With this, the i th diagonal element of $S_{XX}^{-1}(\omega)$ is given by

$$\begin{aligned} \left\{ S_{XX}^{-1}(\omega) \right\}_{ii} &\triangleq S^{ii}(\omega) = \frac{1}{S_{V_i}(\omega)} \frac{|G_i(\omega)|^2 S_u(\omega) / S_{V_i}^2(\omega)}{\left[1 + \sum_{j=1}^M (S/N)_j \right]} \\ &= \frac{1}{S_{V_i}(\omega)} \left[1 - \frac{(S/N)_i}{1 + \sum_{j=1}^M (S/N)_j} \right] \end{aligned} \quad (4.12)$$

or

$$S^{ii}(\omega) = \frac{1}{S_{V_i}(\omega)} \frac{\left[1 + \sum_{i=1}^M (S/N)_j - (S/N)_i \right]}{\left[1 + \sum_{j=1}^M (S/N)_j \right]} \quad (4.13)$$

Using this and substituting equation 4.1 into equation 2.3, we find

$$\begin{aligned} |\gamma_{i/1,2, \dots, i-1, i+1, \dots, M}|^2 &= 1 - 1 / \left(S_{ii}(\omega) S^{ii}(\omega) \right) \\ &= 1 - \frac{\left[1 + \sum_{j=1}^M (S/N)_j \right]}{\left[1 + (S/N)_i \right] \left[1 + \sum_{j=1}^M (S/N)_j - (S/N)_i \right]} \\ &= \frac{(S/N)_i \left[\left(\sum_{j=1}^M (S/N)_j \right) - (S/N)_i \right]}{\left[1 + (S/N)_i \right] \left[1 + \left(\sum_{j=1}^M (S/N)_j \right) - (S/N)_i \right]} \end{aligned} \quad (4.14)$$

Several special cases are of interest.

First consider the situation in which the signal-to-noise ratios in all channels are the same:

$$(S/N)_i = (S/N)_j = (S/N). \quad (4.15)$$

This gives the coherence of channel i with respect to the other $M-1$ channels as

$$|\gamma_{i:1,2,\dots,i-1,i+1,\dots,M}|^2 = \frac{(S/N)^2 (M-1)}{[1 + (S/N)][1 + (M-1)(S/N)]}. \quad (4.16)$$

Note that for M equal to two as in section 3 the coherence is given by

$$|\gamma_{1:2}| = |\gamma_{2:1}| = \frac{(S/N)^2}{[1 + (S/N)]^2}. \quad (4.17)$$

However, if M becomes very large, the coherence goes to

$$|\gamma_{i:1,2,\dots,i-1,i+1,\dots,M}|^2 \rightarrow \frac{S/N}{[1 + (S/N)]}. \quad (4.18)$$

The formal requirement for this to be valid is for the signal-to-noise ratio and number of channels to satisfy the following inequality:

$$(M-1)(S/N) \gg 1. \quad (4.19)$$

However, based on data from section 3, equation 4.18 is identical to the coherence of two channels when one has an infinite signal-to-noise ratio and the other has a signal-to-noise ratio (at frequency ω) of (S/N) . In this sense, a large enough number of weak channels [signal-to-noise ratio of (S/N)] is equivalent to the sum of one noise-free channel and one weak channel.

The second special case for equation 4.14 is when the i th channel has a very large signal-to-noise ratio. Letting $(S/N)_i$ become large in equation 4.14 and keeping all other signal-to-noise ratios equal to (S/N) we find that

$$|\gamma_{i:1,2,\dots,i-1,i+1,\dots,M}|^2 \xrightarrow{(S/N)_i \rightarrow \infty} \frac{(M-1)(S/N)}{[1 + (M-1)(S/N)]}. \quad (4.20)$$

Note that for low signal-to-noise ratios, *i.e.*,

$$(M-1)(S/N) \ll 1, \quad (4.21)$$

the coherence goes up linearly with the number of channels. Each new channel added is also considered to have the same signal-to-noise ratio as all others, *i.e.*, (S/N) . As M becomes larger or as

$$M(S/N) \gg 1, \quad (4.22)$$

this coherence goes to one as it would in the case of two noise-free channels.

The relationships between signal-to-noise ratios and coherence for these two cases are in table 4.1. Note that as expected the signal-to-noise ratio required in each channel to obtain a given coherence declines with an increasing number of channels and increases with an increased level in the specified coherence.

Table 4.1. Signal-to-Noise Power Ratios.

$ \gamma(M) ^2$		Signal-to-Noise Power Ratios Required to Yield Indicated $ \gamma ^2$ Value When All Input Channels Have Equal Signal-to-Noise Ratios					
		0.01	0.05	0.1	0.3	0.5	0.9
M =	2	0.111 -9.5 dB	0.288 -5.4 dB	0.462 -3.3 dB	1.21 0.83 dB	2.41 3.8 dB	18.5 12.6 dB
M =	3	0.079 -11.0 dB	0.206 -6.9 dB	0.333 -4.9 dB	0.885 -0.5 dB	1.78 2.5 dB	13.8 11.4 dB
M =	4	0.065 -11.9 dB	0.172 -7.6 dB	0.280 -5.5 dB	0.760 -1.2 dB	1.55 1.9 dB	12.2 10.9 dB
M =	5	0.057 -12.4 dB	0.152 -8.18 dB	0.250 -6.0 dB	0.691 -1.6 dB	1.42 1.52 dB	11.4 10.6 dB
M =	10	0.040 -14.0 dB	0.111 -9.55 dB	0.189 -7.2 dB	0.561 -2.5 dB	1.20 0.79 dB	10.1 10.0 dB
M =	100	0.016 -18.0 dB	0.060 -12.2 dB	0.121 -9.17 dB	0.443 -3.5 dB	1.02 0.09 dB	9.10 9.6 dB
$ \gamma(M) ^2$		Signal-to-Noise Power Ratios Required to Yield Indicated $ \gamma ^2$ Value When <i>i</i> th Channel Has Infinite Signal-to-Noise Ratio and Other (M-1) Channels Have Indicated Signal-to-Noise Ratios					
		0.01	0.05	0.1	0.3	0.5	0.9
M =	2	0.010 -20.0 dB	0.053 -12.8 dB	0.111 -9.6 dB	0.429 -3.7 dB	1.00 0.0 dB	9.00 9.5 dB
M =	3	0.005 -23.0 dB	0.026 -15.9 dB	0.056 -12.5 dB	0.214 -6.7 dB	0.5 -3.0 dB	4.5 6.5 dB
M =	4	0.003 -25.2 dB	0.017 -17.7 dB	0.037 -14.3 dB	0.143 -8.5 dB	0.333 -4.8 dB	3.0 4.8 dB
M =	5	0.002 -27.0 dB	0.013 -18.9 dB	0.028 -15.5 dB	0.107 -9.7 dB	0.25 -6.0 dB	2.25 3.5 dB
M =	10	0.001 -30.0 dB	0.006 -22.2 dB	0.012 -19.2 dB	0.048 -13.2 dB	0.111 -9.8 dB	1.00 0.0 dB
M =	100	0.0001 -40.0 dB	0.0005 -33.0 dB	0.0011 -29.6 dB	0.0043 -23.7 dB	0.0101 -20.0 dB	0.091 -10.4 dB

Next consider the case where one channel other than the *i*th channel has a very high signal-to-noise ratio relative to the others:

$$(S/N)_k \gg \sum_{j=1}^M (S/N)_j - (S/N)_i - (S/N)_k. \quad (4.23)$$

Under these conditions, equation 4.14 is approximately given by

$$|\gamma_{i:1,2,\dots,i-1,i+1,\dots,M}|^2 \sim \frac{(S/N)_i(S/N)_k}{[1+(S/N)_i][1+(S/N)_k]} \quad (4.24)$$

or

$$|\gamma_{i:1,2,\dots,i-1,i+1,\dots,M}|^2 \sim |\gamma_{i:k}|^2, \quad (4.25)$$

as if all other channels were not used. If $(S/N)_i$ is approximately equal to $(S/N)_k$, this means that all weaker channels could be neglected and only the two-channel coherence between the two stronger channels could be used. Also consider the case when all channels including the i th have a much lower signal-to-noise ratio than the k th channel, *i.e.*,

$$(S/N)_k \gg (S/N)_i = (S/N) \quad \text{all } i \neq k \quad (4.26)$$

Then, while the coherence of the i th channel given the others is provided by equation 4.24, the coherence of the k th channel given the others is

$$|\gamma_{k:1,2,\dots,k-1,k+1,\dots,M}|^2 = \frac{(M-1)(S/N)_k(S/N)}{[1+(S/N)_k][1+(M-1)(S/N)]}. \quad (4.27)$$

Giving for this case

$$\begin{aligned} & |\gamma_{k:1,2,\dots,k-1,k+1,\dots,M}|^2 \\ &= \frac{(M-1)[1+(S/N)]}{[1+(M-1)(S/N)]} |\gamma_{i:1,2,\dots,i-1,i+1,\dots,M}|^2. \end{aligned} \quad (4.28)$$

For the case of weak signals in the other channels (from equation 4.25):

$$|\gamma_{k:1,2,\dots,k-1,k+1,\dots,M}|^2 = \frac{(M-1)(1+S/N)}{[1+(M-1)(S/N)]} |\gamma_{i:k}|^2. \quad (4.29)$$

Further simplifying equation 4.29 to the special case of

$$(M-1)(S/N) \ll 1, \quad (4.30)$$

we have

$$\left| \gamma_{k:1,2,\dots,k-1,k+1,\dots,M} \right|^2 \sim (M-1) \left| \gamma_{i:k} \right|^2. \quad (4.31)$$

The coherence between the strong signal and the weaker ones goes up linearly with the number of weaker channels. This means that the largest of the M multiple coherence values will be the one in which the largest signal-to-noise ratio channel is used as the reference, which is as expected.

SECTION 5.0 A SAMPLE STATISTIC FOR MULTIPLE COHERENCE

As in the case of pairwise coherence discussed in section 3, the true multiple coherence of a set of time series is a function of the underlying statistics of these processes. These statistics are generally unknown and must be estimated from sample realizations of the processes. The estimates of the basic statistics can then be used to provide estimates of the multiple coherence of the M underlying stochastic processes.

The method of obtaining estimates for true multiple coherence is as follows. Using well documented techniques (see references 3, 4, 5, and 6), obtain sample estimates for each element of the crosspower spectral density matrix (equation 2.1). From these sample estimates

$$\hat{S}_{\underline{X}\underline{X}}(\omega) = \begin{bmatrix} \hat{S}_{11}(\omega) & \hat{S}_{12}(\omega) & \dots & \hat{S}_{1M}(\omega) \\ \hat{S}_{21}(\omega) & \hat{S}_{22}(\omega) & \dots & \hat{S}_{2M}(\omega) \\ \cdot & \cdot & \cdot & \cdot \\ \cdot & \cdot & \cdot & \cdot \\ \hat{S}_{M1}(\omega) & \hat{S}_{M2}(\omega) & \dots & \hat{S}_{MM}(\omega) \end{bmatrix} \quad (5.1)$$

one calculates the sample estimate for multiple coherence in the following manner

$$|\bar{\gamma}_{i:1,2,\dots,i-1,i+1,\dots,M}|^2 = 1 - 1/[\hat{S}_{ii}(\omega)\hat{S}^{ii}(\omega)], \quad (5.2)$$

where $\hat{S}^{ii}(\omega)$ is the i th diagonal element of the inverse of the M -by- M sample spectral density matrix $\hat{S}_{\underline{X}\underline{X}}(\omega)$. Details of how to form such estimates are discussed at length in the literature. Since these estimates are random variables there has been considerable study of their distribution. The distributions of these cross- and autopower spectral estimates are known in closed form and are given in reference 7.

SECTION 6.0 DISTRIBUTION OF SAMPLE STATISTICS

As it is for the pairwise coherence discussed in reference 8, the closed-form expression for the multiple-coherence statistic described in the last section is available (references 7, 8, and 9). This represents the range of values of the multiple-coherence test statistic and the relative probability of its being in a particular band. All values are of course bounded by zero and one. The density function is conditioned on the total number of different time records, or different stochastic processes, available (p). It is also conditioned on the number of independent complex samples available from each of the time records (N) at a given frequency w . Thus from reference 9 the density function of the sample estimate for coherence given the true coherence is given by

$$\begin{aligned}
 P_{|\gamma|^2}(y/N, p, |\gamma|^2) &= \frac{\Gamma(N)}{\Gamma(p-1)\Gamma(N-p+1)} (1-|\gamma|^2)^N y^{p-2} (1-y)^{N-p} \\
 &\cdot {}_2F_1(N, N, p-1; y|\gamma|^2) \\
 0 \leq y \leq 1
 \end{aligned}$$

$$P_{|\gamma|^2}(y/N, p, |\gamma|^2) = 0 \quad y > 1 \text{ or } y < 0. \tag{6.1}$$

In equation 6.1, ${}_2F_1(\)$ is the hypergeometric function (reference 10).

This expression for the density function of multiple coherence is both expensive to calculate and generally numerically ill conditioned. Thus to evaluate the density numerically, additional manipulations are required. Great difficulty can be encountered in attempting to use computer library expressions for the hypergeometric function.

For low values of N and p we can use a transformation given in reference 12:

$$\begin{aligned}
 {}_2F_1(N, N, p-1; |\gamma|^2 y) &= (1-|\gamma|^2 y)^{p-1-2N} {}_2F_1(p-1-N, p-1-N, p-1; |\gamma|^2 y). \tag{6.2}
 \end{aligned}$$

For the cases of interest, $(p-1-N)$ is a negative integer so that a finite series expansion for this latter hypergeometric function is available:

$$\begin{aligned}
& {}_2F_1(N, N, p-1; |\gamma|^2 y) \\
&= (1 - |\gamma|^2 y)^{p-1-2N} \sum_{j=0}^{N-p+1} \frac{(-N+p-1)_j^2}{(p-1)_j} \frac{(|\gamma|^2 y)^j}{j!}, \tag{6.3}
\end{aligned}$$

where

$$(p-1)_j = (p+j-1)!/(p-1)! = (p+j-2)(p+j-3) \dots (p-1) \tag{6.4}$$

$$(-N+p-1)_j = (-N+p-1)(-N+p) \dots (-N+p-2+j). \tag{6.5}$$

Using these expressions for the hypergeometric function we can write for y between zero and one:

$$\begin{aligned}
P_{|\gamma|^2} (y/N, p, |\gamma|^2) &= \frac{\Gamma(N)(1-|\gamma|^2)^N}{\Gamma(p-1)\Gamma(N-p+1)} \\
&\cdot \frac{y^{p-2}(1-y)^{N-p}}{(1-|\gamma|^2 y)^{2N-(p-1)}} \sum_{j=0}^{N-(p-1)} \frac{[-N+(p-1)]_j^2}{(p-1)_j} \frac{(|\gamma|^2 y)^j}{j!}. \tag{6.6}
\end{aligned}$$

An alternative expression can be derived by using the relationship between hypergeometric functions and Jacobi polynomials. Thus,

$$P_n^{\alpha, \beta}(x) = \binom{n+\alpha}{n} \left(\frac{1+x}{2}\right)^n {}_2F_1\left(-n, -n-\beta, \alpha+1; \frac{x-1}{x+1}\right) \tag{6.7}$$

(from reference 12). Using this identity and letting

$$\beta = 0$$

$$\alpha = p-2$$

$$n = N-(p-1)$$

$$(x-1)/(x+1) = |\gamma|^2 y \text{ or } x = (1 + |\gamma|^2 y)/(1 - |\gamma|^2 y), \tag{6.8}$$

we have

$$\begin{aligned}
& {}_2F_1(p-N-1, p-N-1, p-1; |\gamma|^2 y) \\
&= \frac{(1-|\gamma|^2 y)^{N-(p-1)}}{\binom{N-1}{N-(p-1)}} P_{N-(p-1)}^{p-2, 0} [(1+|\gamma|^2 y)/(1-|\gamma|^2 y)]. \tag{6.9}
\end{aligned}$$

Using the general expansion for the Jacobi polynomial

$$P_n^{\alpha, \beta}(x) = \frac{\Gamma(\alpha+n+1)}{n! \Gamma(\alpha+\beta+n+1)} \sum_{m=0}^n \binom{n}{m} \frac{\Gamma(\alpha+\beta+n+m+1)}{\Gamma(\alpha+m+1)} \left(\frac{x-1}{2}\right)^m, \quad (6.10)$$

we find that

$$\begin{aligned} & P_{N-p+1}^{p-2, 0} [(1+|\gamma|^2 y)/(1-|\gamma|^2 y)] \\ &= \frac{1}{[N-(p-1)]!} \sum_{m=0}^{N-(p-1)} \binom{N-(p-1)}{m} \frac{\Gamma(N+m)}{\Gamma(m+p-1)} \left[\frac{|\gamma|^2 y}{1-|\gamma|^2 y} \right]^m \end{aligned} \quad (6.11)$$

so that another general expression for this conditional density of the coherence is

$$\begin{aligned} P \frac{y}{|\gamma|^2} (y | N, p, |\gamma|^2) &= \left[\frac{1-|\gamma|^2}{1-y|\gamma|^2} \right]^N \frac{y^{p-2} (1-y)^{N-p}}{(N-p)!} \\ & \sum_{m=0}^{N-(p-1)} \binom{N-p+1}{m} \frac{(N+m-1)!}{(m+p-2)!} \left[\frac{(|\gamma|^2 y)}{(1-|\gamma|^2 y)} \right]^m. \end{aligned} \quad (6.12)$$

When true coherence is zero this reduces to

$$P \frac{y}{|\gamma|^2} (y | N, p, |\gamma|^2 = 0) = \frac{y^{p-2} (1-y)^{N-p} (N-1)!}{(p-2)! (N-p)!} \quad (6.13)$$

and for two channels to

$$P \frac{y}{|\gamma|^2} (y | N, p=2, |\gamma|^2 = 0) = (N-1)(1-y)^{N-2}. \quad (6.14)$$

To calculate receiver operating characteristics it is necessary to evaluate integrals of these densities. To do this analytically, we expand the term $(1-y)^{N-p}$

$$\begin{aligned} P \frac{y}{|\gamma|^2} (y | N, p, |\gamma|^2) &= \left[\frac{(1-|\gamma|^2)^N}{(N-p)!} \right] \\ & \sum_{m=0}^{N-(p-1)} \binom{N-p+1}{m} \frac{(N+m-1)!}{(m+p-2)!} |\gamma|^{2m} \sum_{j=0}^{N-p} (-1)^j \binom{N-p}{j} \frac{y^{m+j+p-2}}{(1-|\gamma|^2 y)^{N+m}}. \end{aligned} \quad (6.15)$$

It is easily seen that

$$\begin{aligned} & \int_0^r y^{M/(1-|\gamma|^2y)} L dy \\ &= (1/|\gamma|^2)^{M+1} \sum_{j=0}^M (-1)^j \binom{M}{j} \left[(1-|\gamma|^2r)^{M-L-j+1} - 1 \right] / (M-L-j+1) \end{aligned} \quad (6.16)$$

so that the distribution function of the estimate for the coherence can be written as

$$\begin{aligned} F_{|\gamma|^2} (y | N, p, |\gamma|^2) &= \int_0^y P_{|\gamma|^2} (r | N, p, |\gamma|^2) dr \\ &= \frac{(1-|\gamma|^2)^N}{(N-p)!} \sum_{m=0}^{N-(p-1)} \binom{N-p-1}{m} \sum_{j=0}^{N-p} (-1)^j \binom{N-p}{j} \frac{1}{|\gamma|^{2(j+p-1)}} \\ &\quad \cdot \sum_{s=0}^{m+j+p-2} \frac{(-1)^s \binom{m+j+p-2}{s}}{(-N+j+p-1-s)} \left[(1-|\gamma|^2y)^{-N+j+p-1-s} - 1 \right], \end{aligned} \quad (6.18)$$

which will be numerically well behaved for (large) values of $|\gamma|^2$ greater than one-half. Interchanging the order of summation, this can be written as

$$\begin{aligned} F_{|\gamma|^2} (y | N, p, |\gamma|^2) &= \left[\frac{1-|\gamma|^2}{1-|\gamma|^2y} \right]^N \frac{1}{(N-p)! |\gamma|^{2(p-1)}} \\ &\quad \cdot \sum_{s=p-N}^{N-1} \frac{(-1)^{p-s}}{(N-s)} \left[(1-|\gamma|^2y)^s - (1-|\gamma|^2y)^N \right], \end{aligned} \quad (6.19)$$

$$= \sum_{m=\text{MAX}(0, 1-s)}^{N-(p-1)} \binom{N-(p-1)}{m} \sum_{j=\text{MAX}(0, s+1-p)}^{N-p} \binom{N-p}{j} \binom{m+j+p-2}{j+p-1-s} (|\gamma|^2)^{-j}$$

where for given values of N , p , and $|\gamma|^2$ the last two sums can be evaluated independently of y . These values can then be stored to greatly reduce the computation required to evaluate additional integral values for the same values of N , p , and $|\gamma|^2$.

An expression which can be used for small values of $|\gamma|^2$ can be obtained by expanding the term $(1-|\gamma|^2y)^{-L}$ in equation 6.16 to obtain

$$\int_0^r y^m / (1 - |\gamma|^2 y)^L dy = \frac{r^{m+1}}{m+1} \sum_{j=0}^{\infty} \frac{(L+j-1)!}{j!(L-1)!} (|\gamma|^2 r)^j \frac{(m+1)}{(m+1+j)}. \quad (6.20)$$

Using this in equation 6.15 we obtain

$$\begin{aligned} F_{|\gamma|^2}(y | N, p, |\gamma|^2) &= (1 - |\gamma|^2)^N (N-p+1) \\ &\sum_{m=0}^{N-(p-1)} \frac{(N+m-1)!}{m!(N-p-m+1)!} \frac{|\gamma|^{2m}}{(m+p-2)!} \sum_{k=0}^{N-p} (-1)^k \binom{N-p}{k} \frac{y^{k+m+p-1}}{k+m+p-1} \\ &\cdot \sum_{j=0}^{\infty} \frac{(N+m+j-1)!}{j!(N+m-1)!} (|\gamma|^2 y)^j \frac{(k+m+p-1)}{(j+k+m+p-1)}. \end{aligned} \quad (6.21)$$

or by rearranging orders of summation and simplifying we find

$$\begin{aligned} F(y | N, p, |\gamma|^2) &= 1.0 - (1 - |\gamma|^2)^N \sum_{r=0}^{\infty} |\gamma|^{2r} \binom{N+r-1}{r} \binom{N+r-1}{r+p-2} (N-p+1) \\ &\sum_{j=0}^{r+(p-2)} (-1)^j \binom{r+p-2}{j} \frac{(1-y)^{N-p+1+j}}{j+N-p+1}. \end{aligned} \quad (6.22)$$

For true coherence equal to zero this gives

$$\begin{aligned} F(y | N, p, |\gamma|^2 = 0.0) \\ &= 1 - \frac{p(p-1)}{N} \binom{N}{p} \sum_{j=0}^{p-2} \frac{(-1)^j}{N-p+j+1} \binom{p-2}{j} (1-y)^{N-p+1+j}, \end{aligned} \quad (6.23)$$

and for p equal to 2 the distribution function for $|\gamma|^2$ is:

$$F(y | N, p=2, |\gamma|^2 = 0.0) = 1 - (1-y)^{N-1}. \quad (6.24)$$

The density functions of the sample statistic for coherence when the true coherence is zero, the H_0 hypothesis case, are shown in figure 6.1 for a number of degrees of freedom (N) from 1 to 2048. For N greater than 8, densities for the number of sensors (p) equal to 2, 3, 4, 5, and 10 are indicated.

Figures 6.2 through 6.12 show density functions for a given number of degrees of freedom (N) and a given number of channels (p). The density functions of the sample statistic for coherence for the stated values of N and p and for true coherence of 0.0, 0.05, 0.1, 0.3 and 0.9 are given.

Based on these data it is possible to calculate the performance curves for the multiple-coherence statistic as a detection test statistic. This procedure is well documented in a number of textbooks (references 13, 14, and 15). Basically, these performance curves are developed in the following manner. For a given level of true multiple coherence $|\gamma|^2$, number of degrees of freedom, and number of channels, one defines two hypotheses, H_0 and H_1 . Hypothesis H_0 is that there is no causality between the referenced channel and the other channels and thus the coherence is zero. Hypothesis H_1 is that there is a causal relationship between the channels (time series) and thus the true multiple coherence is $|\gamma|^2$. For a given threshold (α), hypothesis H_0 is chosen if the sample value of the multiple-coherence statistic is below α and H_1 is chosen if the sample value of the statistic is above α . The probability that H_1 is selected when H_0 is true is the probability of false alarm (P_{FA}):

$$P_{FA}(\alpha) = \int_{\alpha}^1 P_{|\gamma|^2}(y/|\gamma|^2 = 0, N, p) dy.$$

The probability that H_1 is selected when H_1 is valid is the probability of detection (P_{DET}):

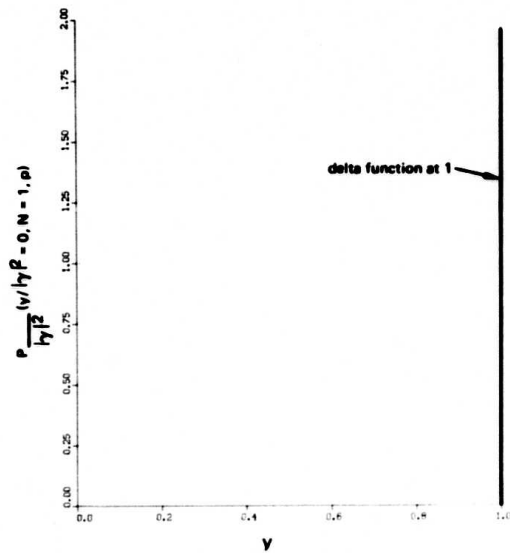
$$P_{DET}(\alpha) = \int_{\alpha}^1 P_{|\gamma|^2}(y/|\gamma|^2, N, p) dy.$$

For each value of N and p we can plot $P_{DET}(\alpha)$ as a function of $P_{FA}(\alpha)$, since α runs from 0 to 1. These curves are in figures 6.13 through 6.18 for N of 32, 64, 128, 512, and 1024; parts a through e correspond to the number of channels. Curves for several values of true coherence are indicated.

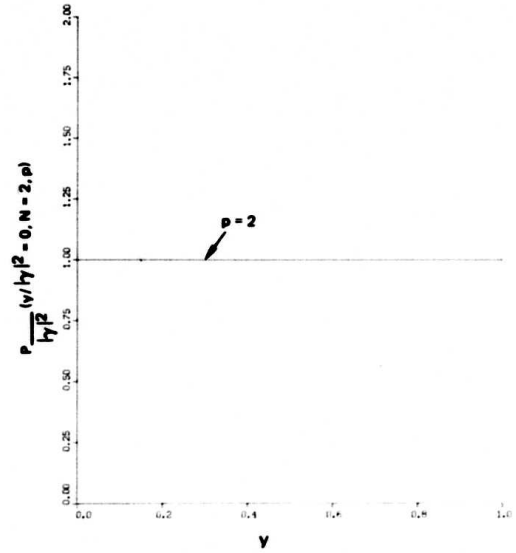
The difficulty with these classical performance curves is that they are linear in probability of false alarm and therefore do not properly illustrate low values for this parameter. This is alleviated by plotting the same data with a log scale used as the probability of false alarm (figures 6.19 through 6.24).

In using multiple coherence as a detection test statistic, the value for true coherence is not generally known. Thus it is of interest to determine how the probability of detection varies for a fixed value for probability of false alarm. This can be determined from figures 6.19 through 6.24 by selecting a given probability of false alarm and drawing a vertical line from which the probability of detection as a function of true coherence can be determined.

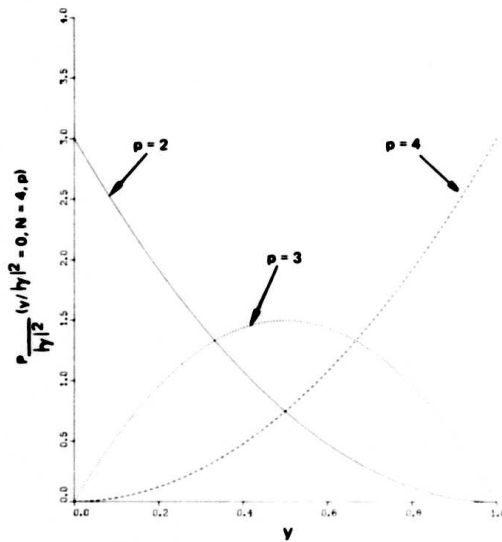
Plots for probability of detection as a function of true coherence for values for probability of false alarm (10^{-1} to 10^{-6}) are in figures 6.25 through 6.30.



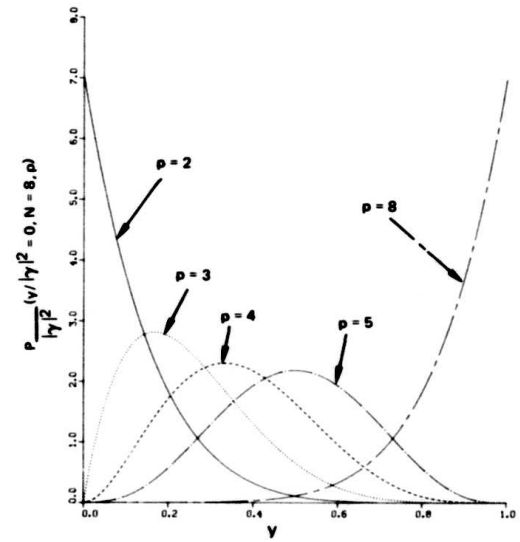
PART A. NUMBER OF DEGREES OF FREEDOM = 1.



PART B. NUMBER OF DEGREES OF FREEDOM = 2.

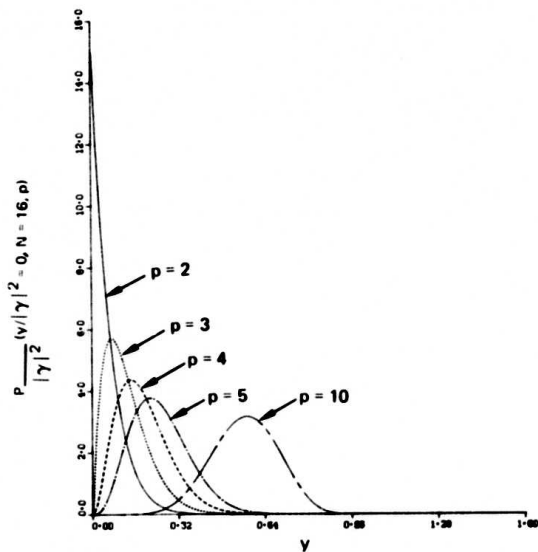


PART C. NUMBER OF DEGREES OF FREEDOM = 4.

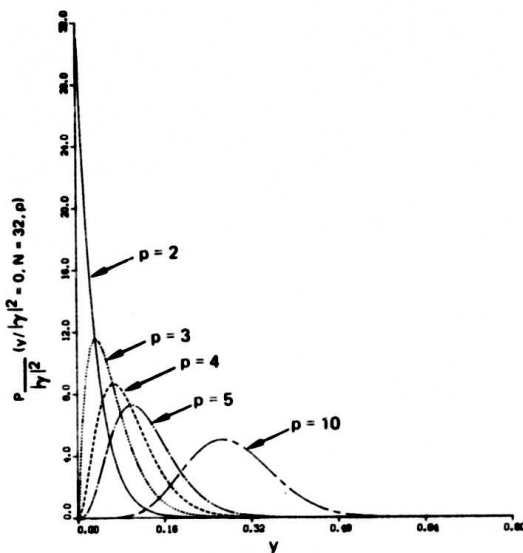


PART D. NUMBER OF DEGREES OF FREEDOM = 8.

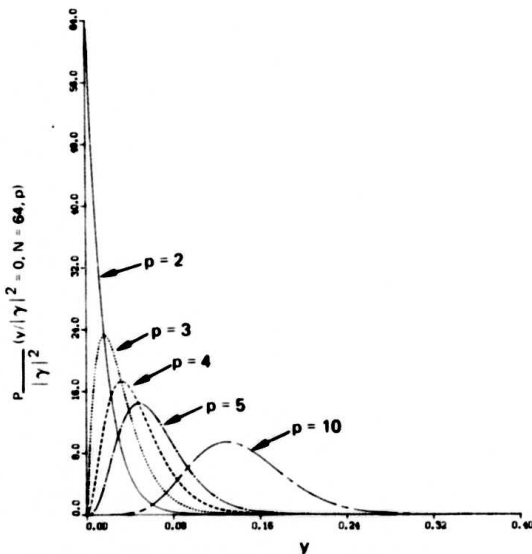
Figure 6.1. Density function of sample statistic for true coherence of zero.



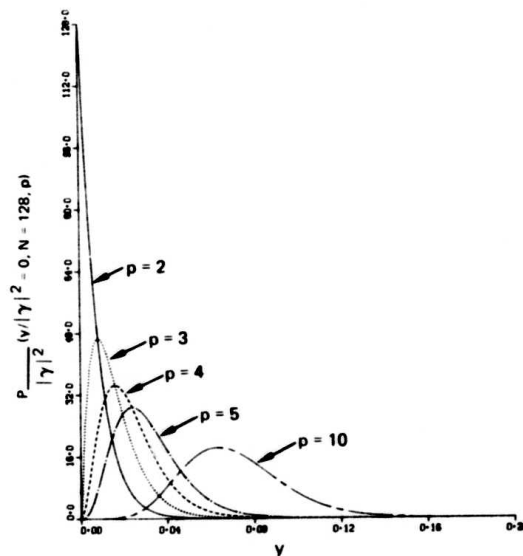
PART E. NUMBER OF DEGREES OF FREEDOM = 16.



PART F. NUMBER OF DEGREES OF FREEDOM = 32.

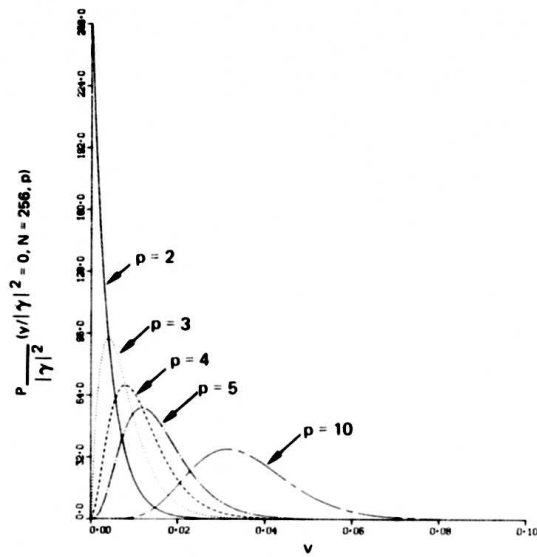


PART G. NUMBER OF DEGREES OF FREEDOM = 64.

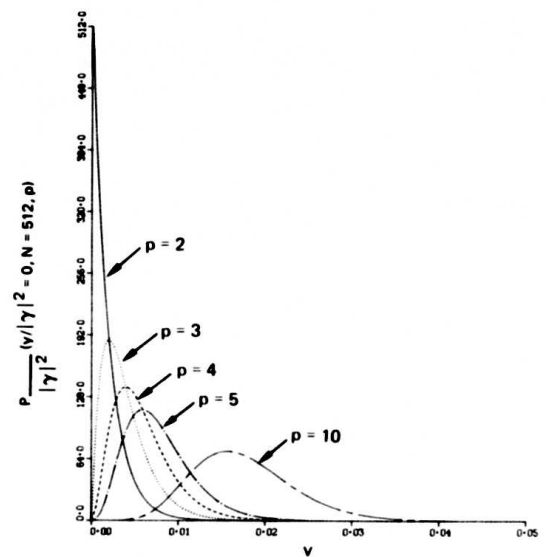


PART H. NUMBER OF DEGREES OF FREEDOM = 128.

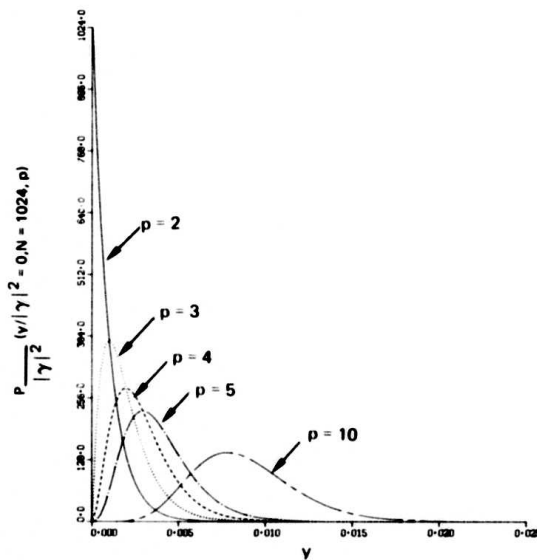
Figure 6.1. (Continued).



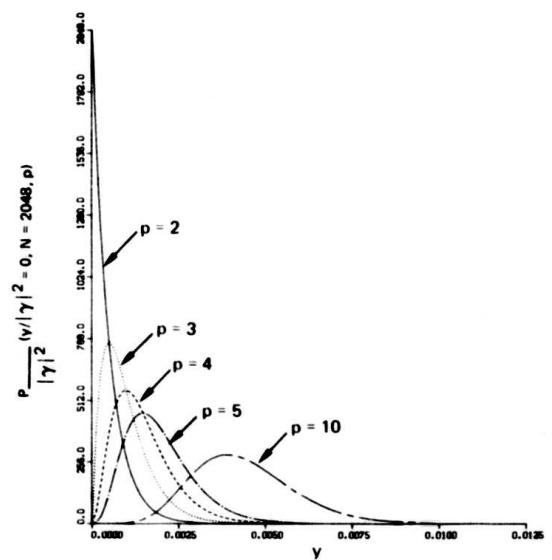
PART I. NUMBER OF DEGREES OF FREEDOM = 256.



PART J. NUMBER OF DEGREES OF FREEDOM = 512.



PART K. NUMBER OF DEGREES OF FREEDOM = 1024.



PART L. NUMBER OF DEGREES OF FREEDOM = 2048.

Figure 6.1. (Continued).

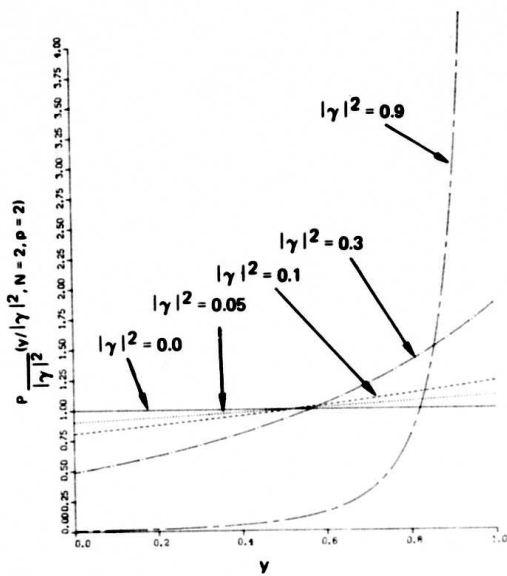
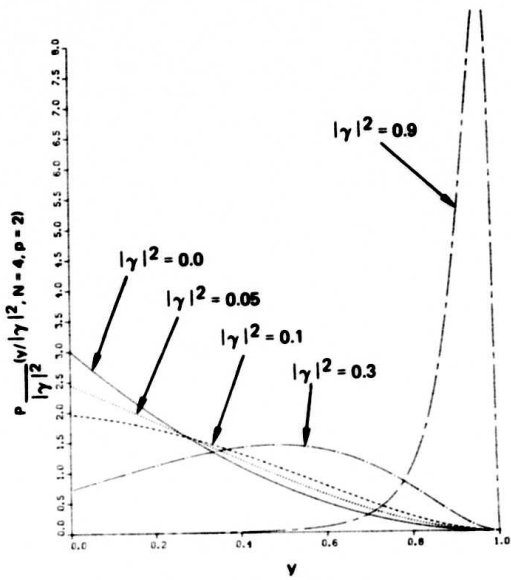
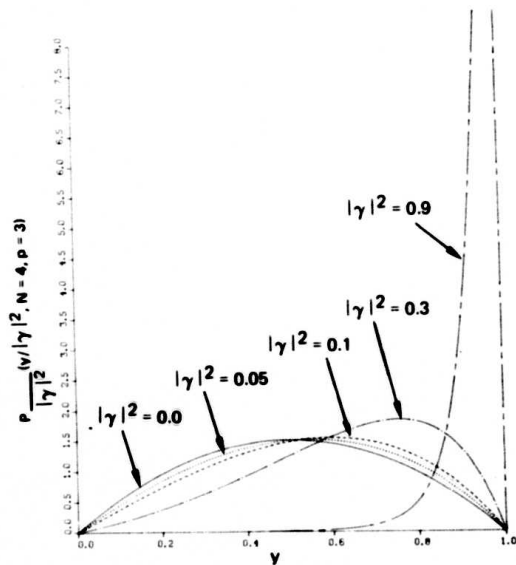


Figure 6.2. Density function for 2 degrees of freedom (N) and 2 channels (p).

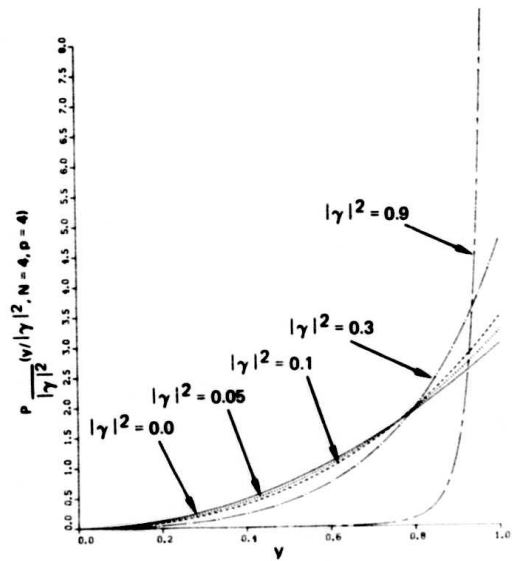


PART A. NUMBER OF CHANNELS (p) = 2.

Figure 6.3. Density functions for 4 degrees of freedom (N).



PART B. NUMBER OF CHANNELS (p) = 3.



PART C. NUMBER OF CHANNELS (p) = 4.

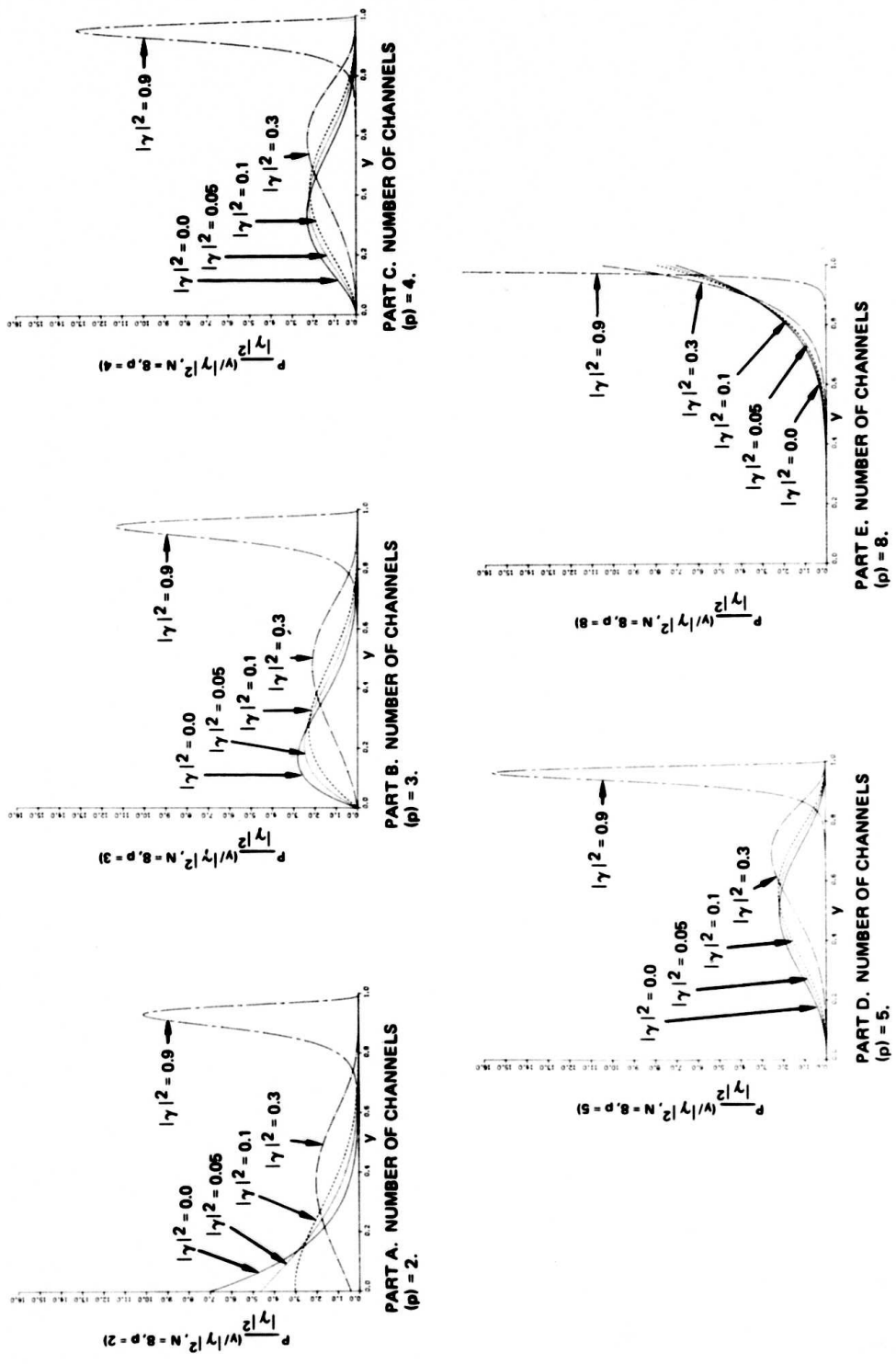


Figure 6.4. Density functions for 8 degrees of freedom (N).

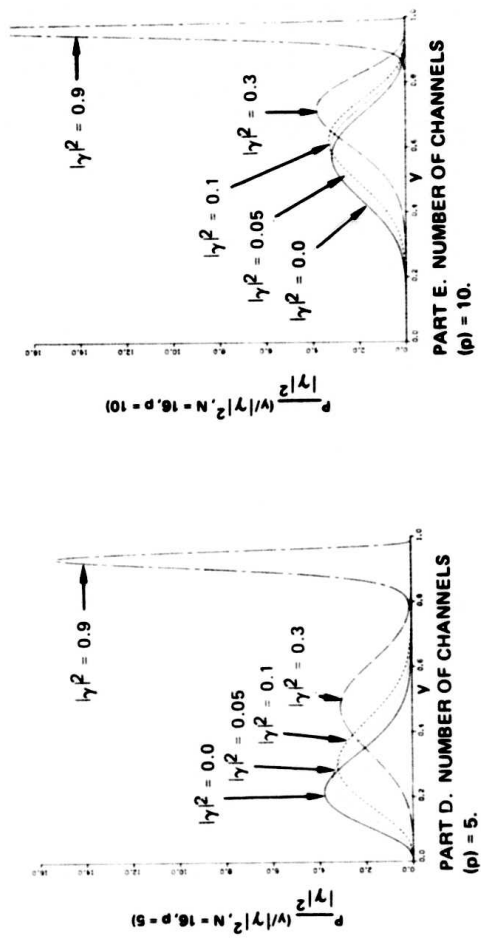
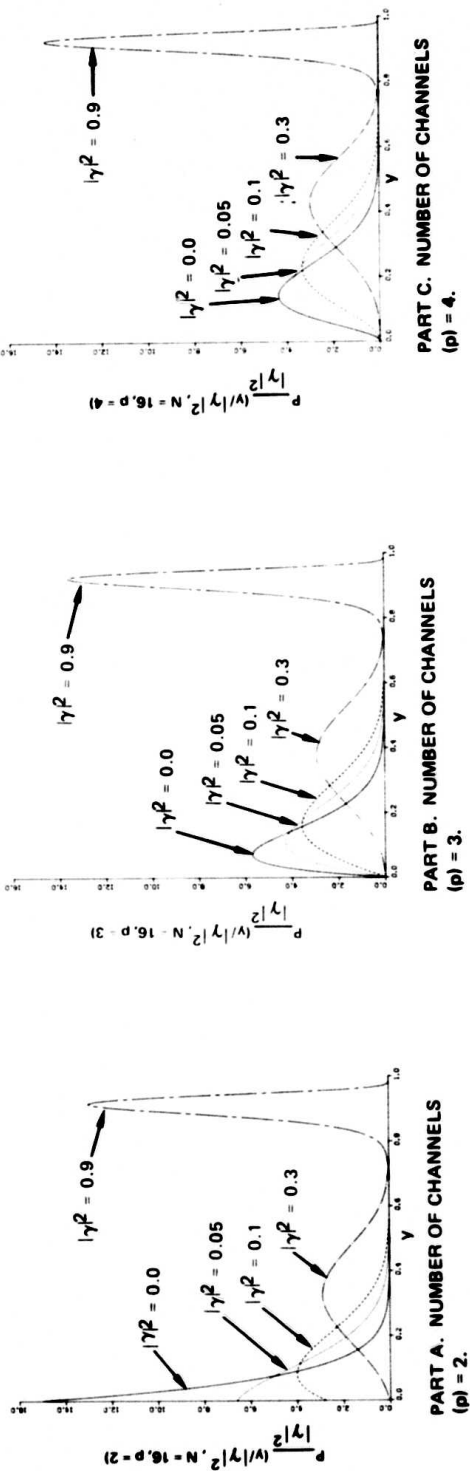


Figure 6.5. Density function for 16 degrees of freedom (N).

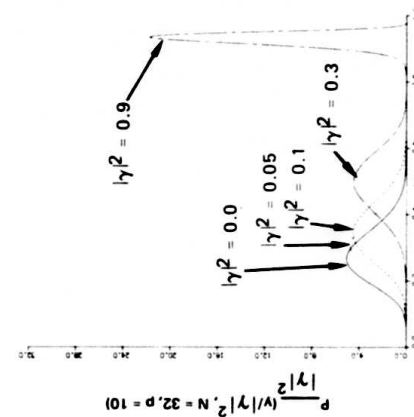
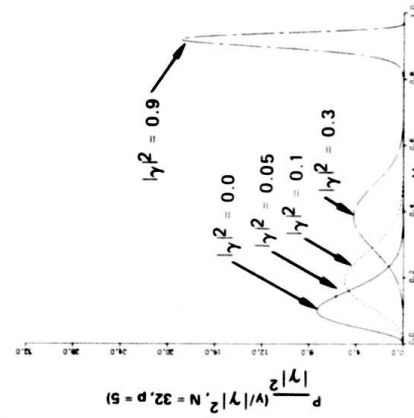
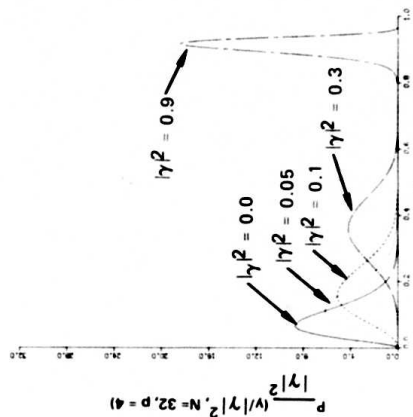
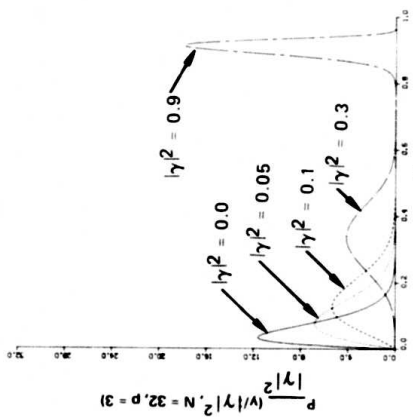
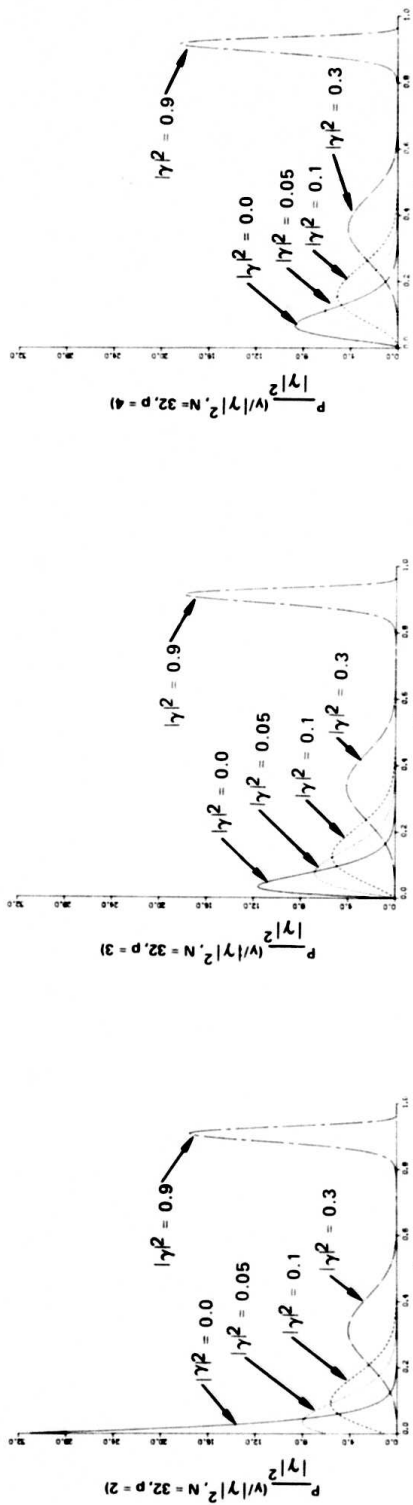


Figure 6.6. Density function for 32 degrees of freedom (N).

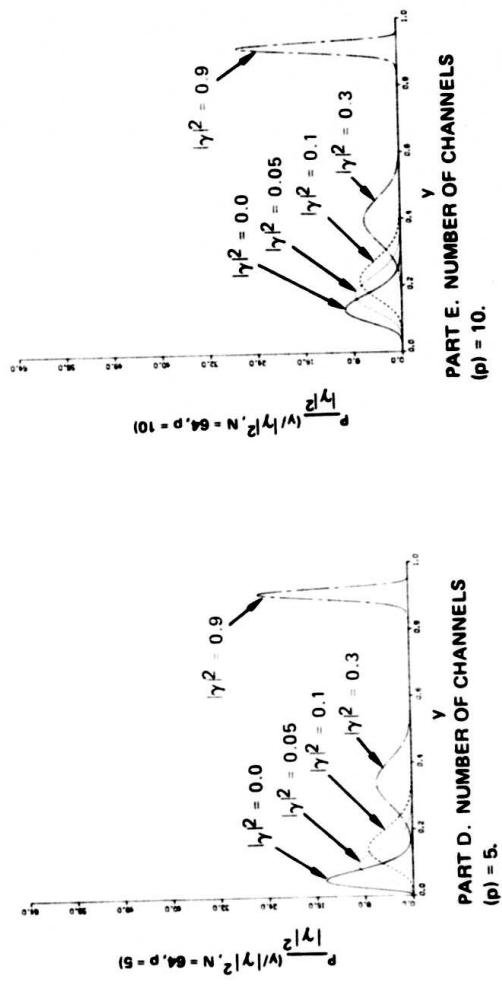
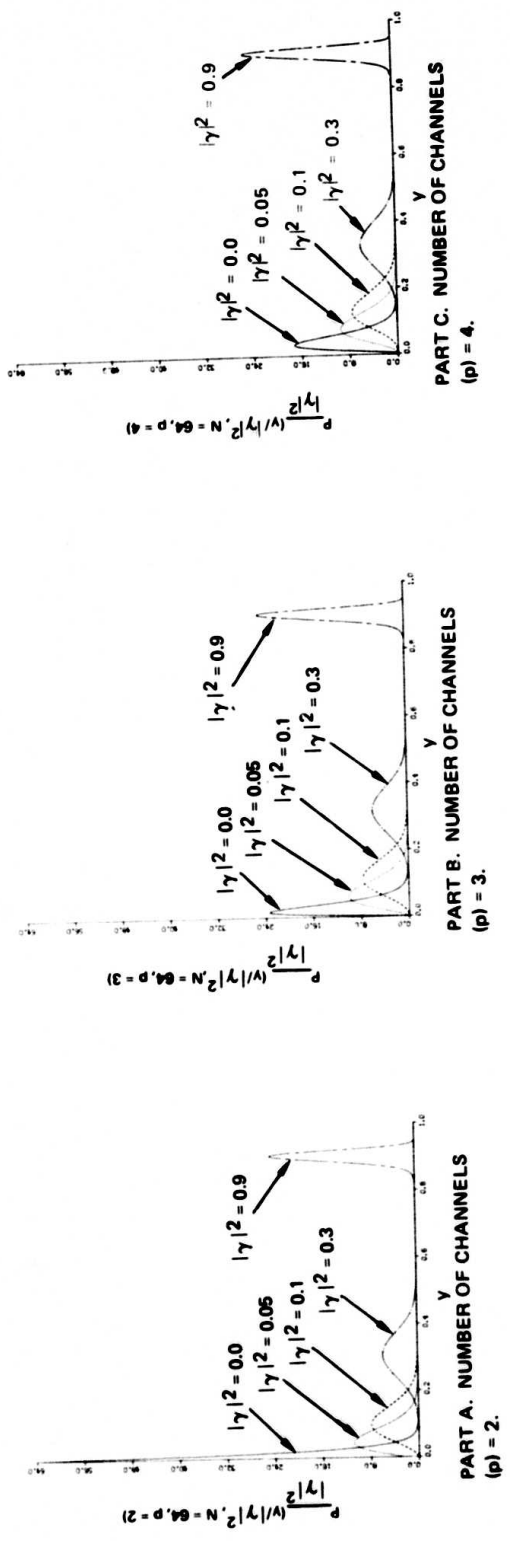


Figure 6.7. Density function for 64 degrees of freedom (N).

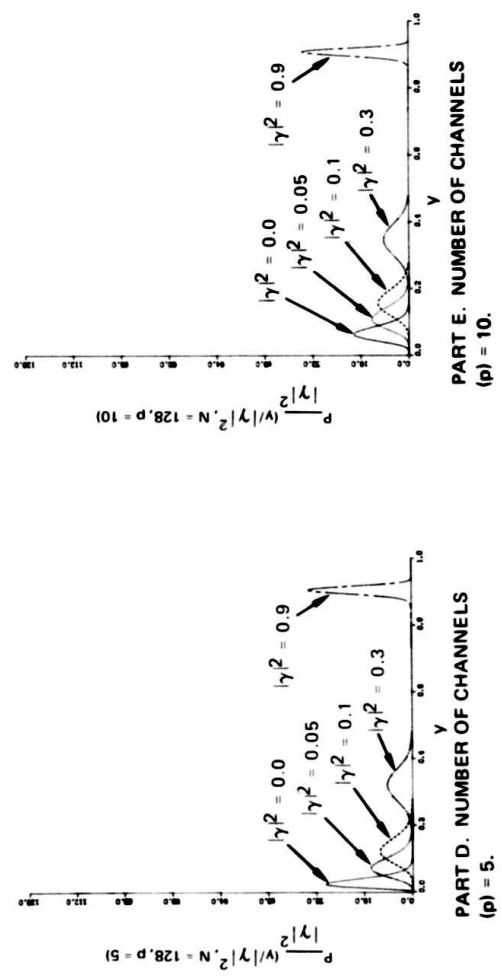
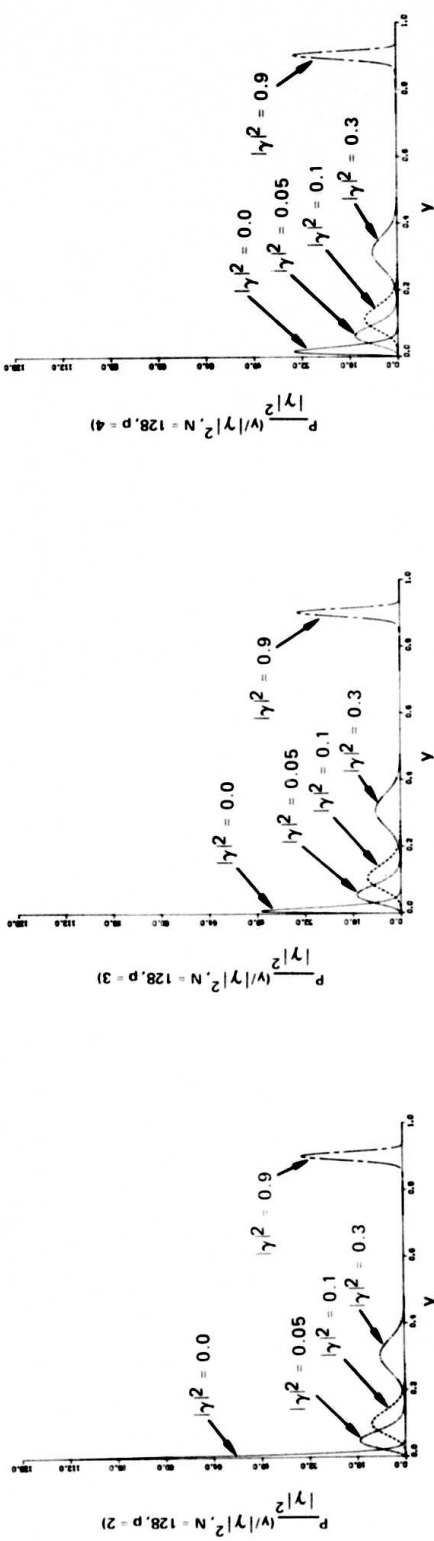


Figure 6.8. Density function for 128 degrees of freedom (N).

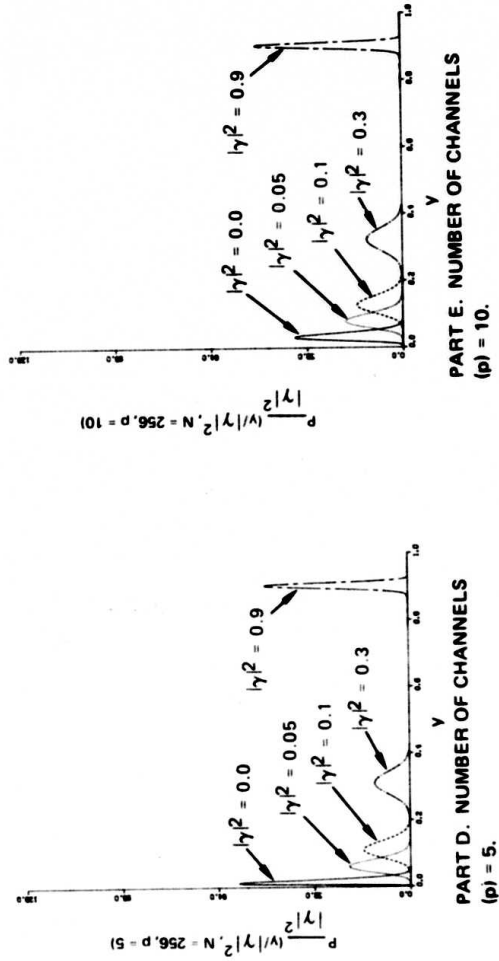
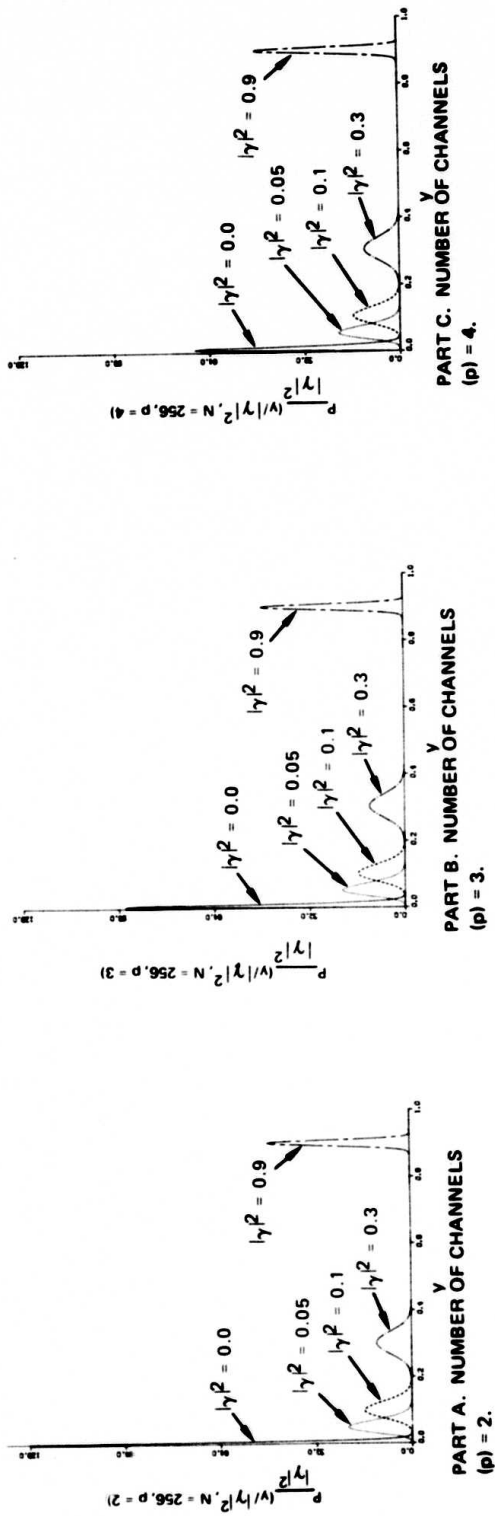


Figure 6.9. Density function for 256 degrees of freedom (N).

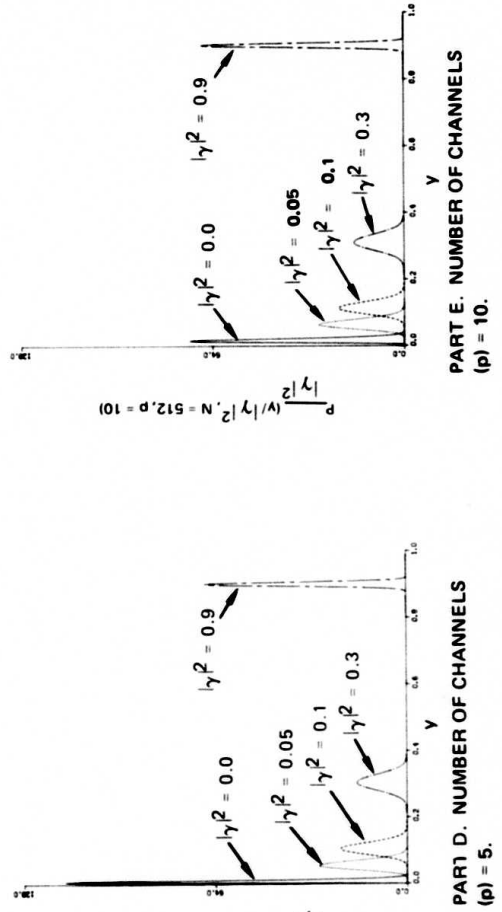
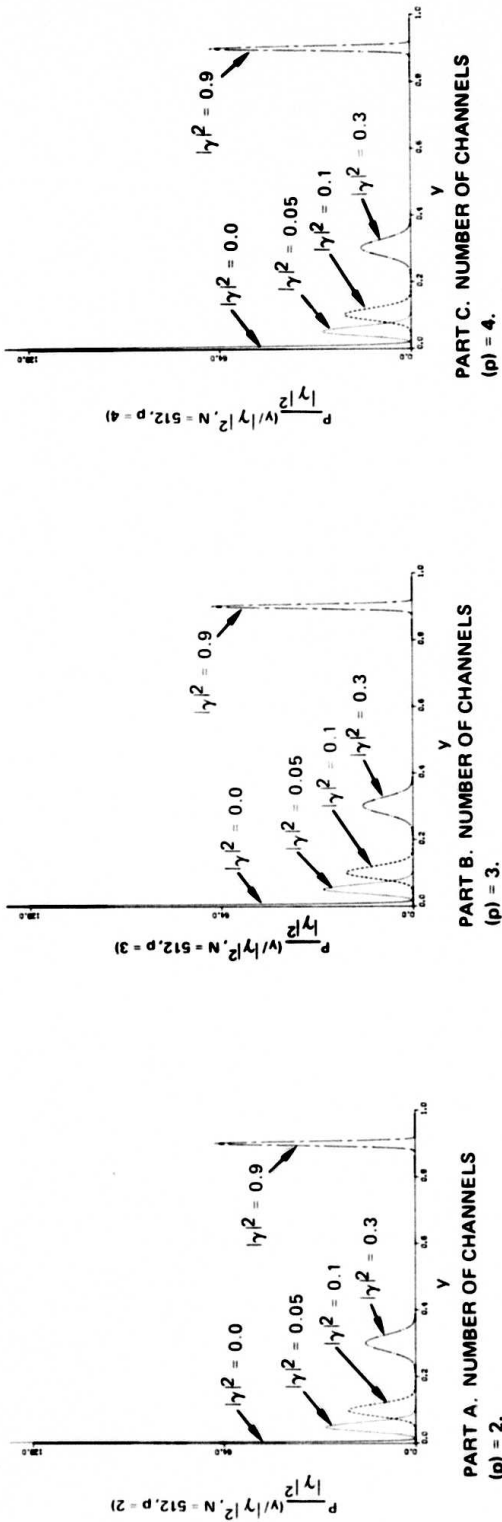


Figure 6.10. Density function for 512 degrees of freedom (N).

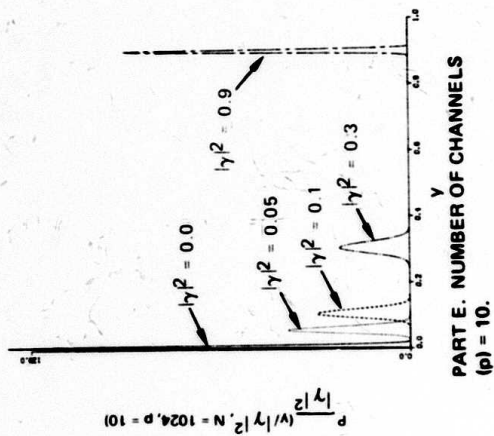
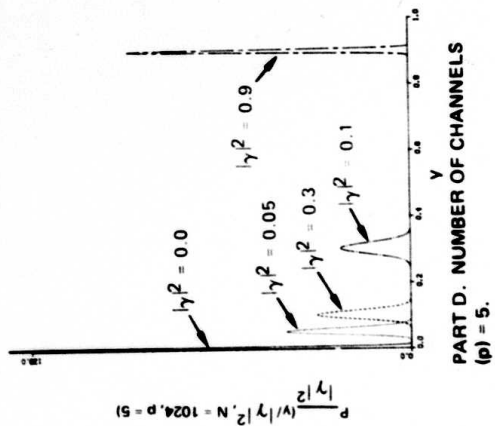
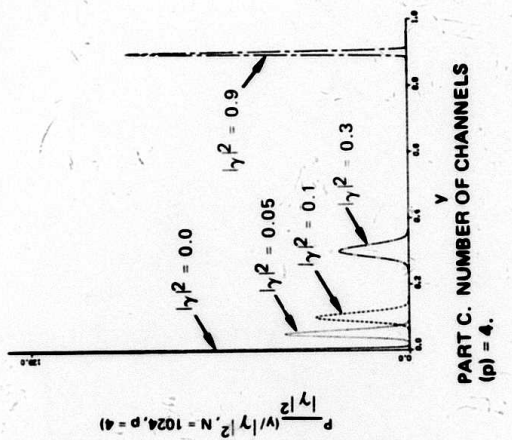
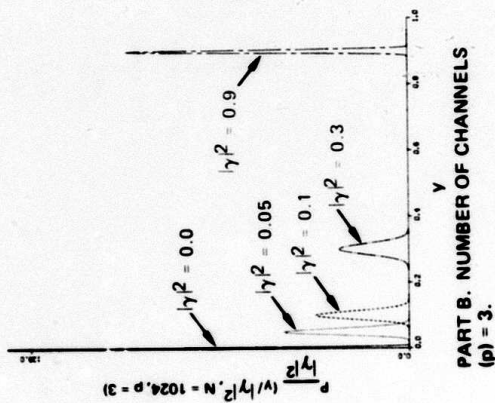
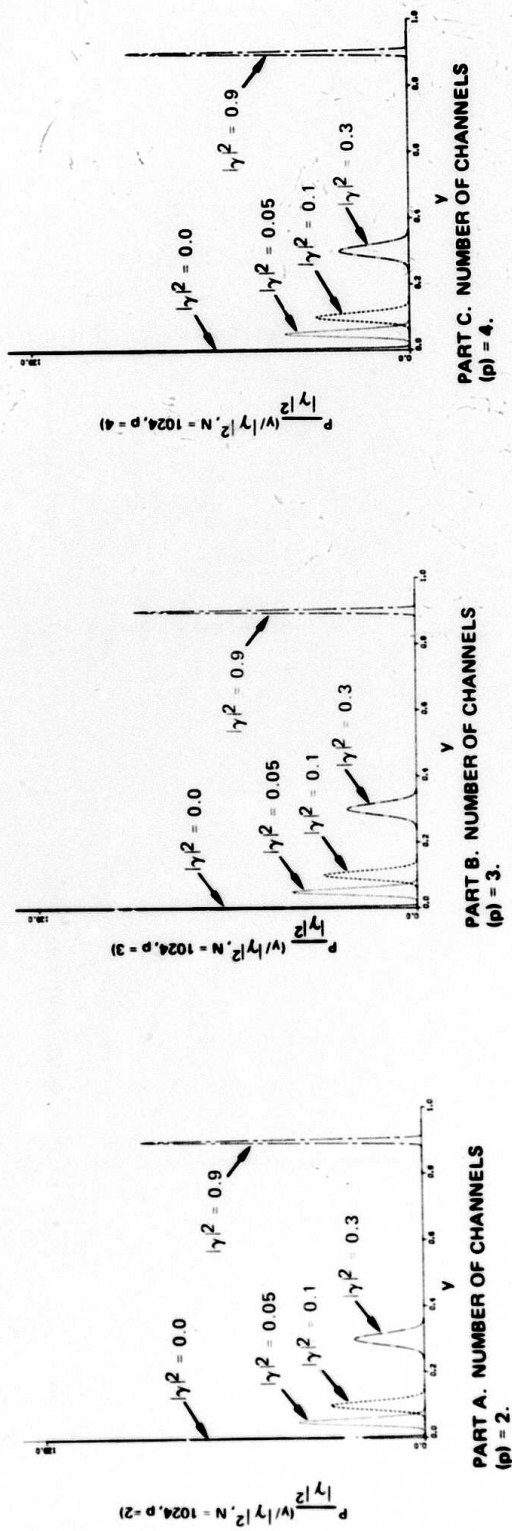


Figure 6.11. Density function for 1024 degrees of freedom (N).

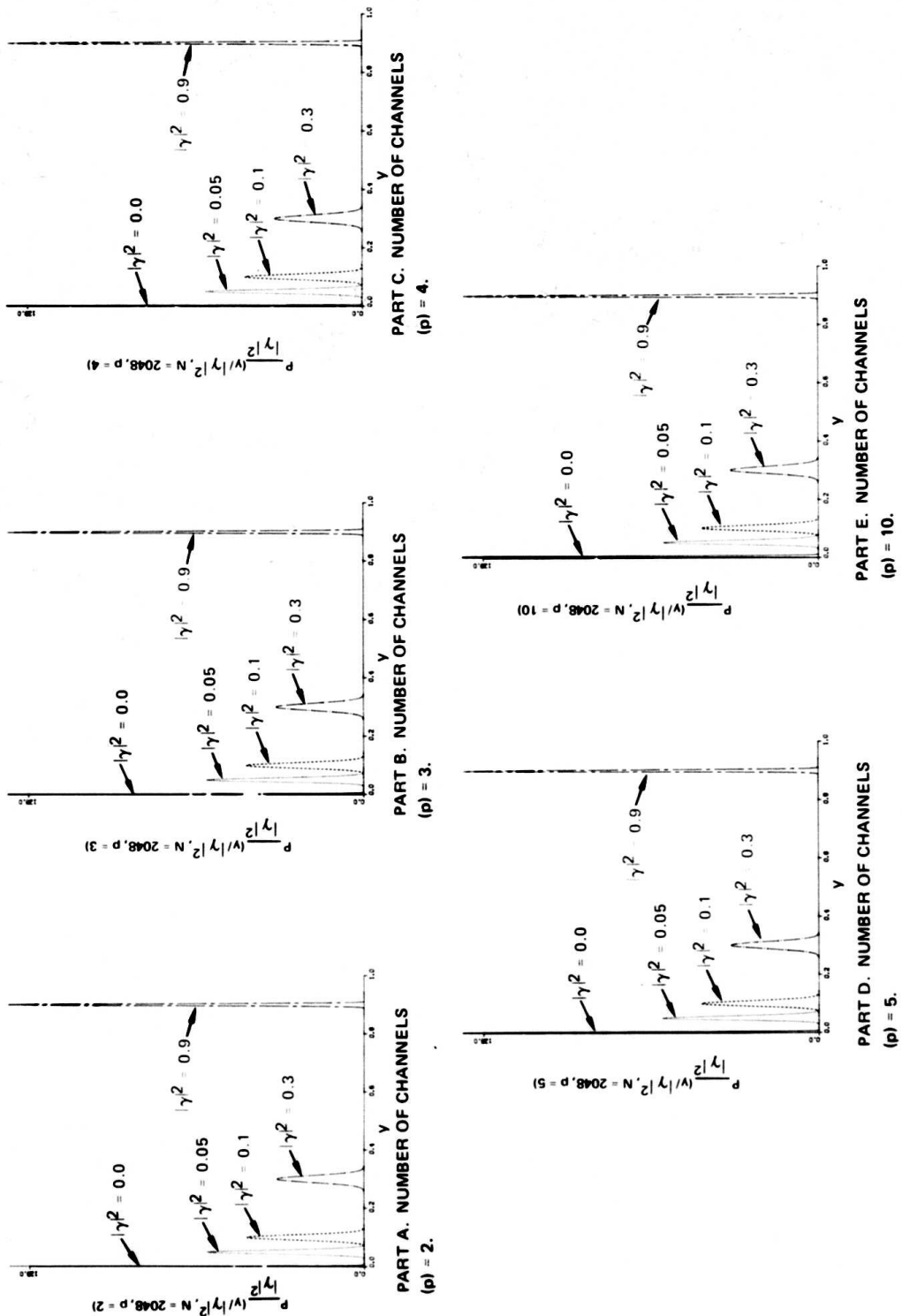


Figure 6.12. Density functions for 2048 degrees of freedom (N).

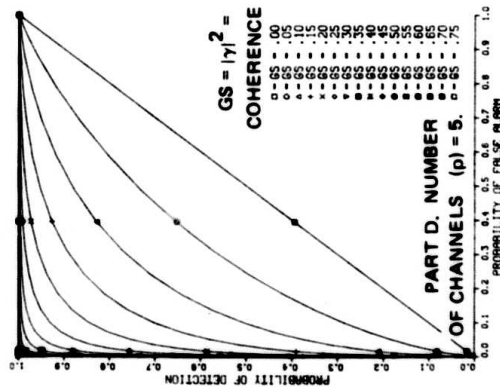
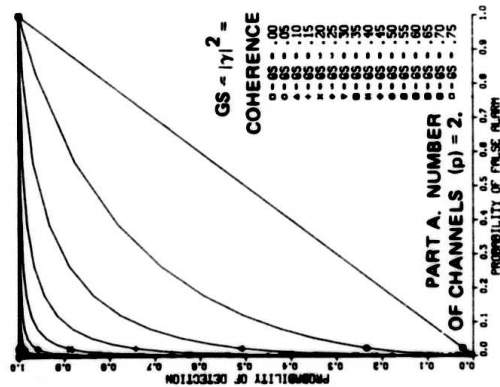
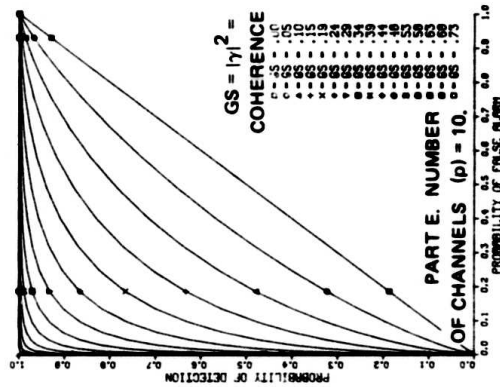
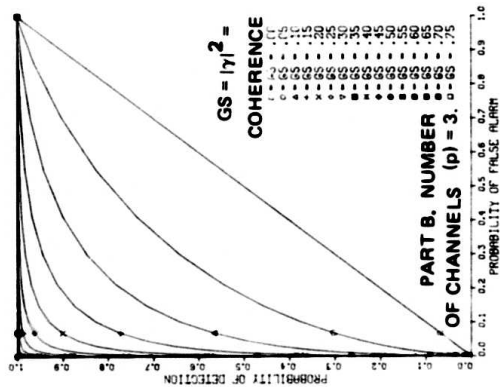
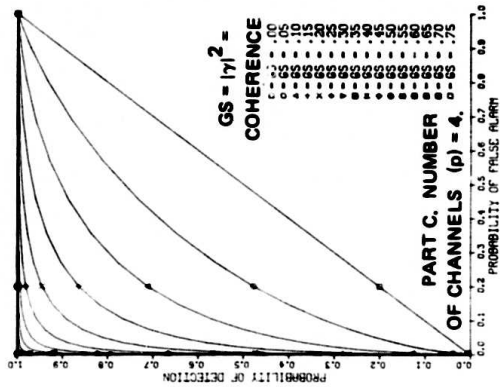


Figure 6.13. Linear receiver operating characteristics: performance curves for the multiple-coherence test statistic. Number of degrees of freedom (N) = 32.

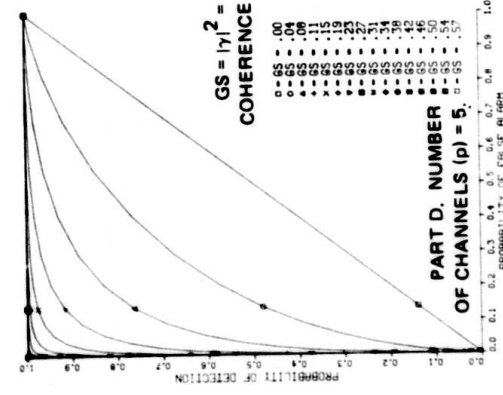
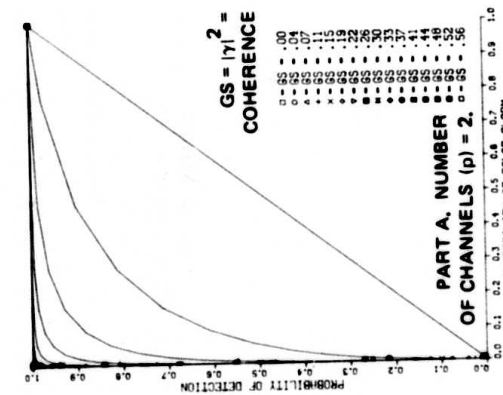
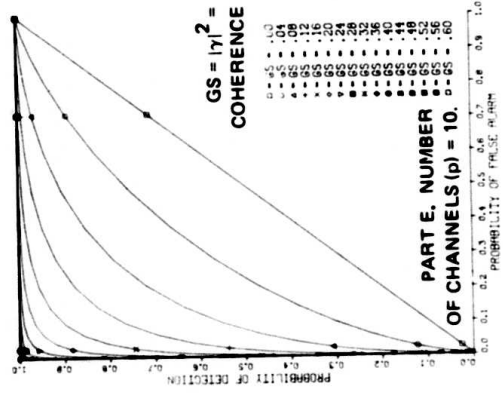
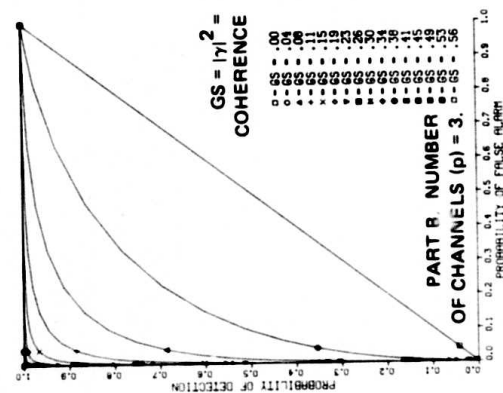
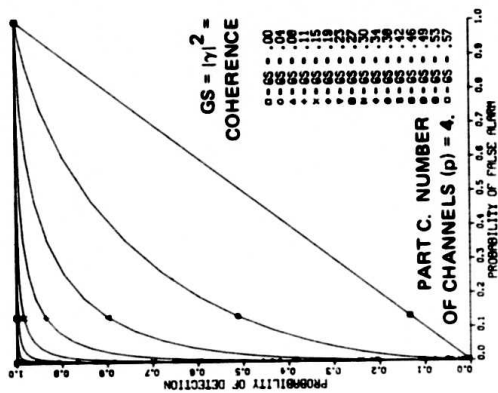


Figure 6.14. Linear receiver operating characteristics: performance curves for the multiple-coherence test statistic. Number of degrees of freedom (N) = 64.

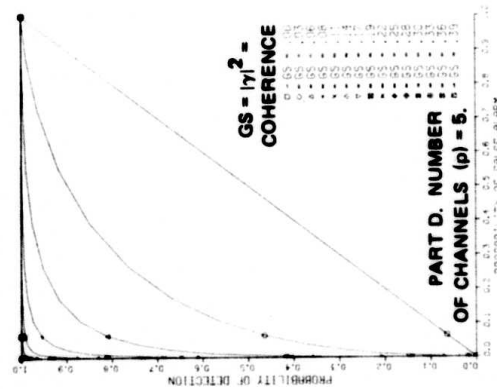
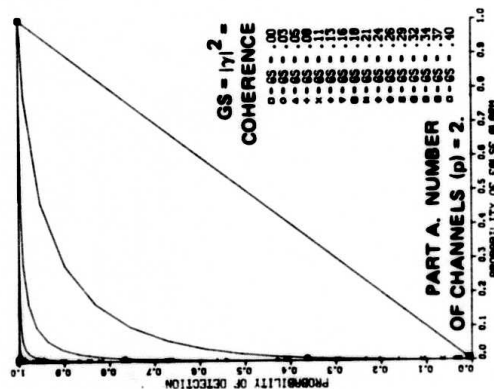
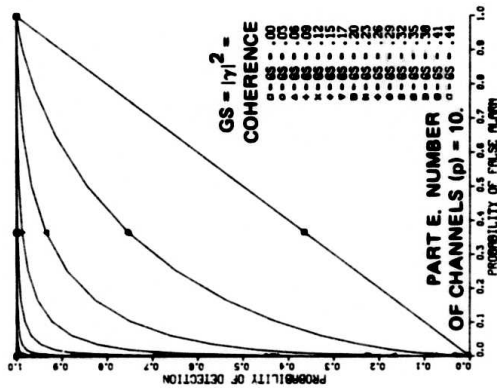
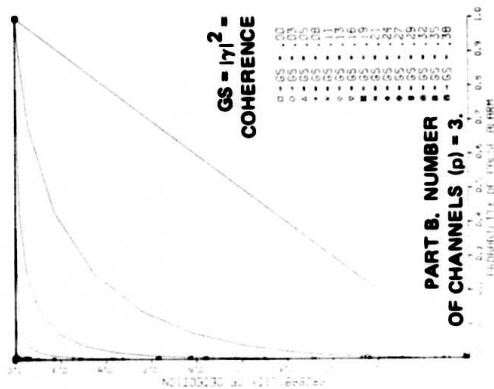
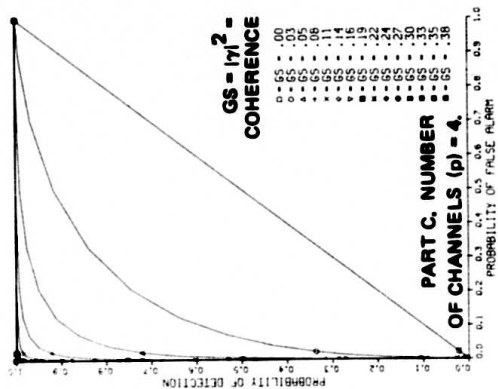


Figure 6.15. Linear receiver operating characteristics: performance curves for the multiple-coherence test statistic. Number of degrees of freedom (N) = 128.

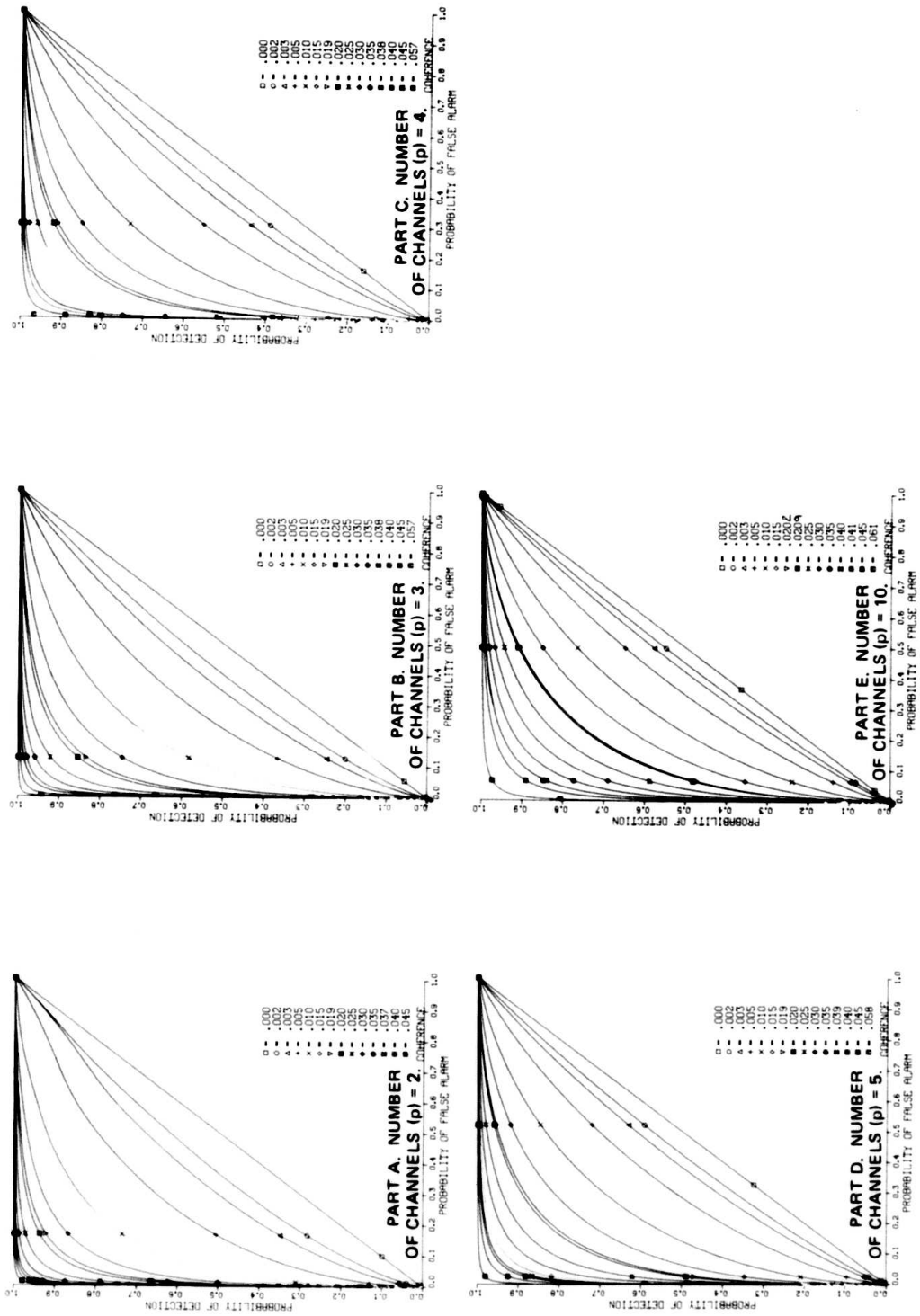


Figure 6.16. Linear receiver operating characteristics: performance curves for the multiple-coherence test statistic. Number of degrees of freedom (N) = 256.

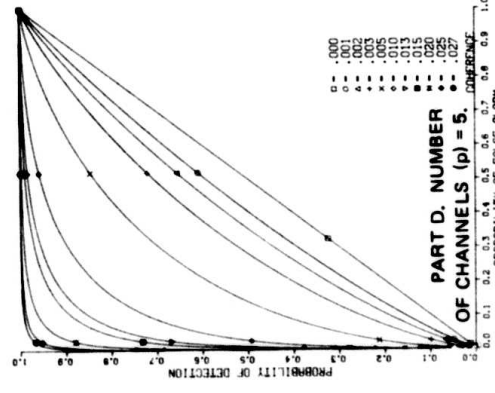
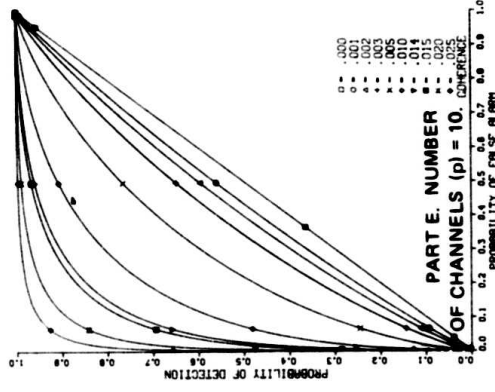
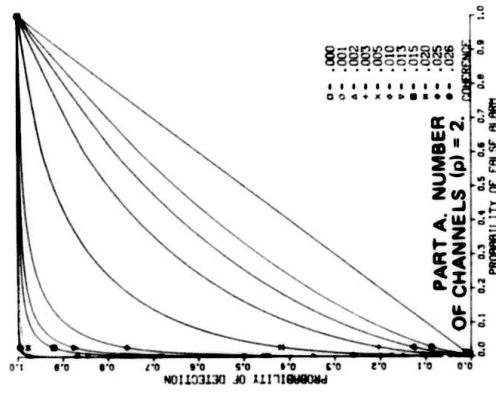
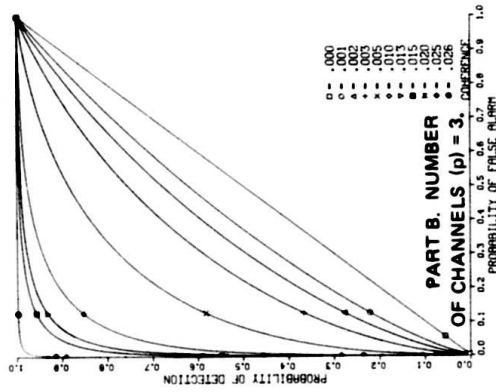
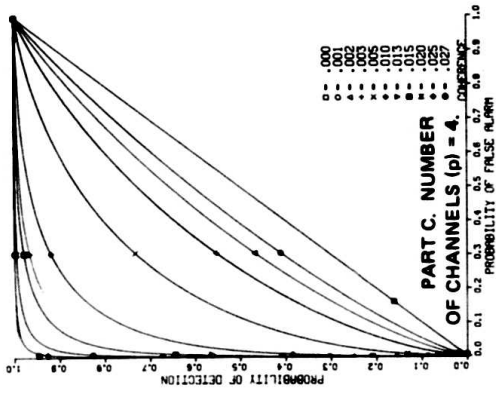


Figure 6.17. Linear receiver operating characteristics: performance curves for the multiple-coherence test statistic. Number of degrees of freedom (N) = 512.

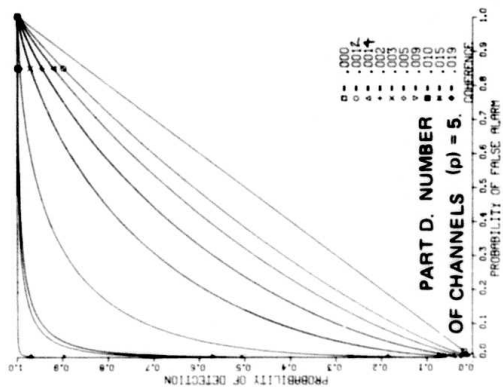
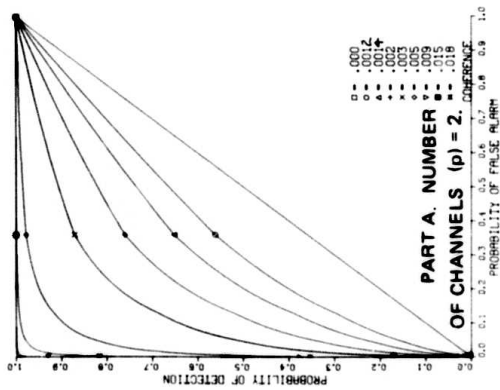
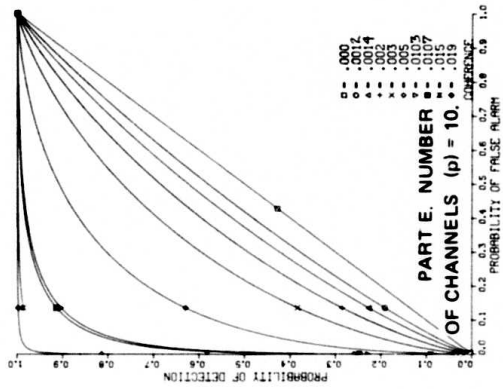
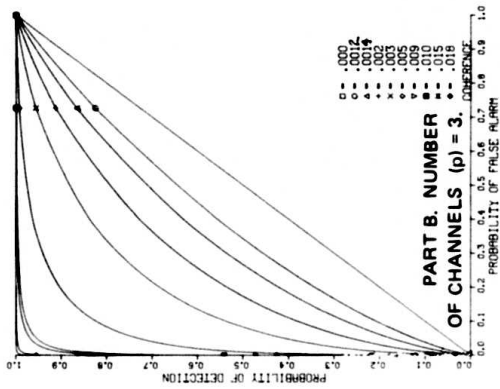
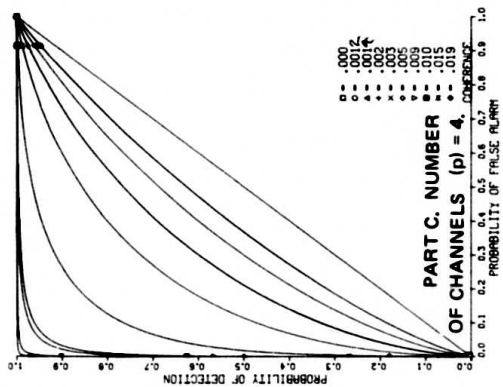
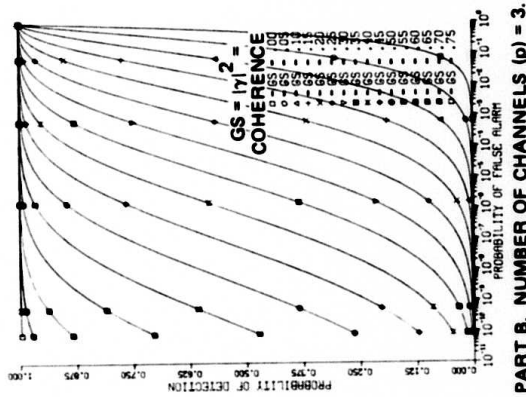
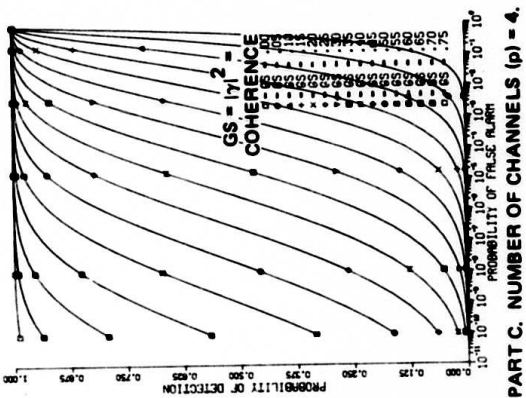


Figure 6.18. Linear receiver operating characteristics: performance curves for the multiple-coherence test statistic. Number of degrees of freedom (N) = 1024.



PART B. NUMBER OF CHANNELS (p) = 3.

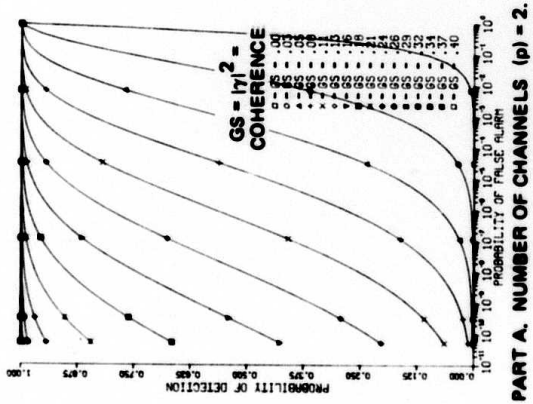
PART A. NUMBER OF CHANNELS (p) = 2.

PART C. NUMBER OF CHANNELS (p) = 4.

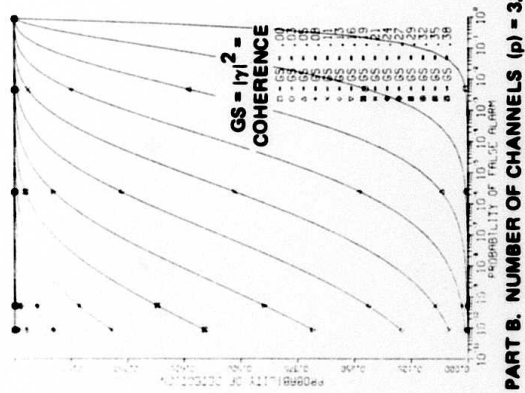
PART D. NUMBER OF CHANNELS (p) = 5.

PART E. NUMBER OF CHANNELS (p) = 10.

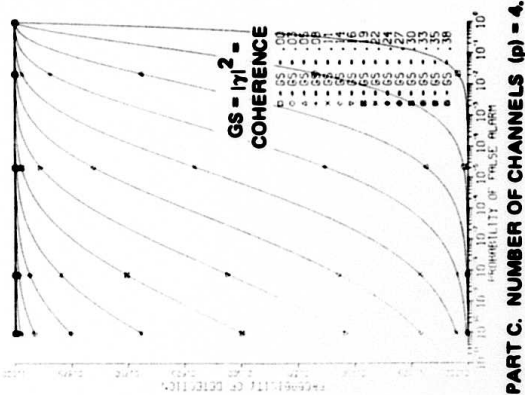
Figure 6.19. Semilog receiver operating characteristics: performance curves for the multiple-coherence test statistic. Number of degrees of freedom (N) = 32.



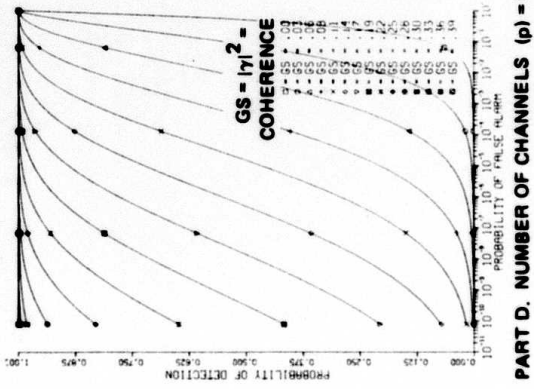
PART A. NUMBER OF CHANNELS (p) = 2.



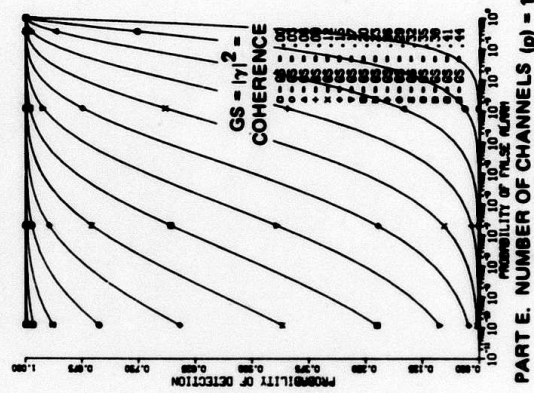
PART B. NUMBER OF CHANNELS (p) = 3.



PART C. NUMBER OF CHANNELS (p) = 4.



PART D. NUMBER OF CHANNELS (p) = 5.



PART E. NUMBER OF CHANNELS (p) = 10.

Figure 6.21. Semilog receiver operating characteristics: performance curves for the multiple-coherence test statistic. Number of degrees of freedom (N) = 128.

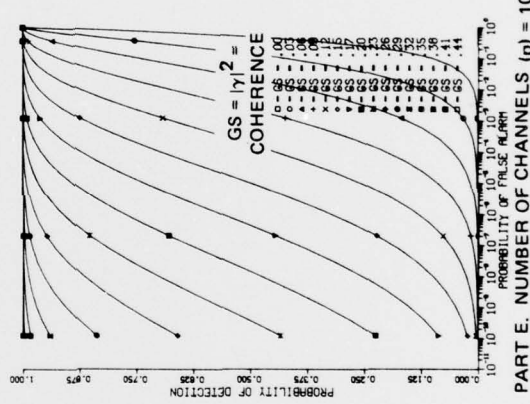
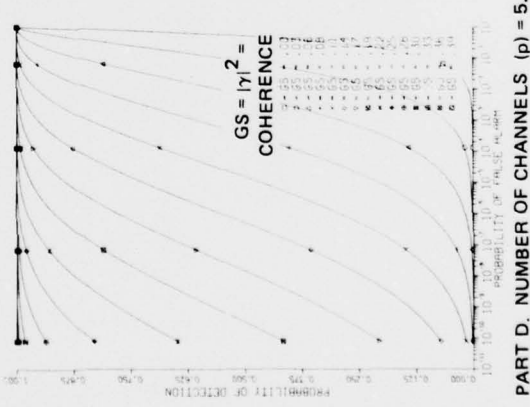
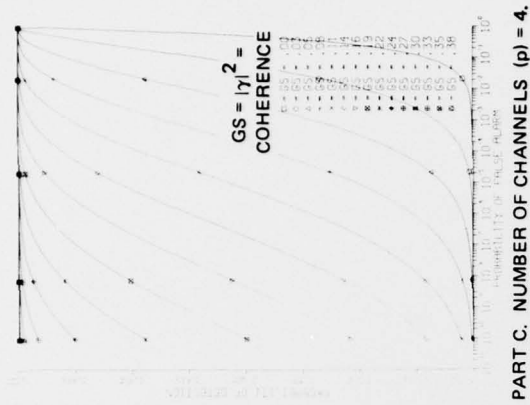
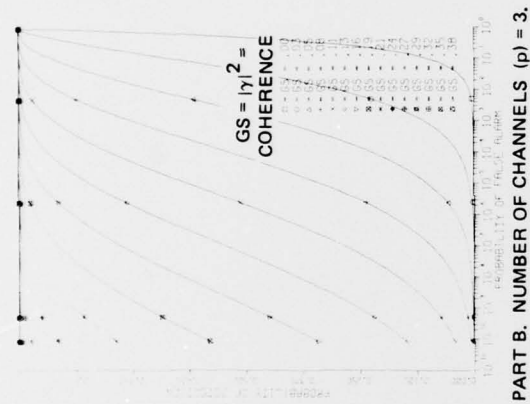
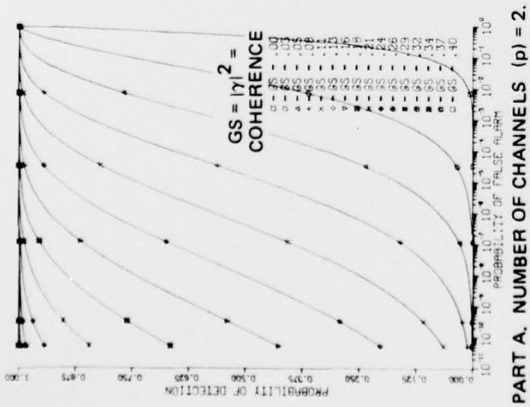
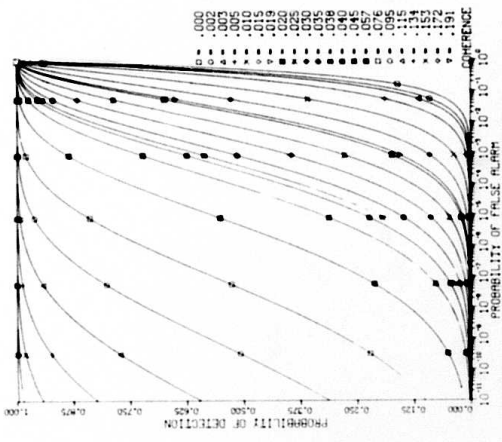
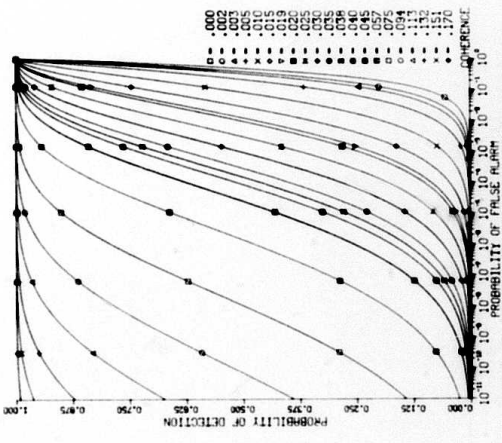


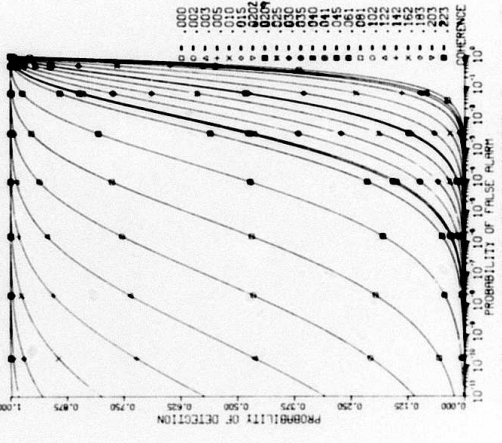
Figure 6.21. Semilog receiver operating characteristics: performance curves for the multiple-coherence test statistic. Number of degrees of freedom (N) = 128.



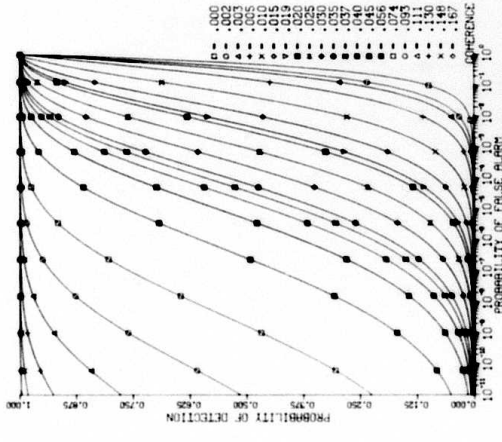
PART C. NUMBER OF CHANNELS (p) = 4.



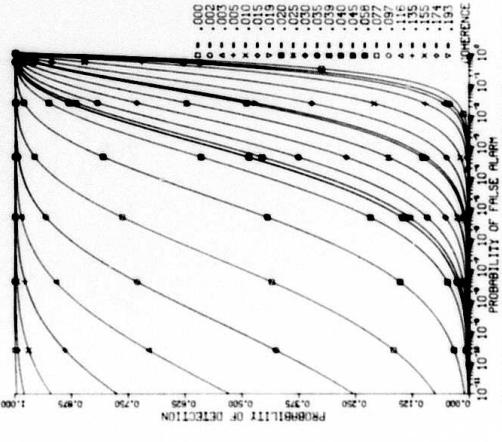
PART B. NUMBER OF CHANNELS (p) = 3.



PART E. NUMBER OF CHANNELS (p) = 10.



PART A. NUMBER OF CHANNELS (p) = 2.



PART D. NUMBER OF CHANNELS (p) = 5.

Figure 6.22. Semilog receiver operating characteristics: performance curves for the multiple-coherence test statistic. Number of degrees of freedom (N) = 256.

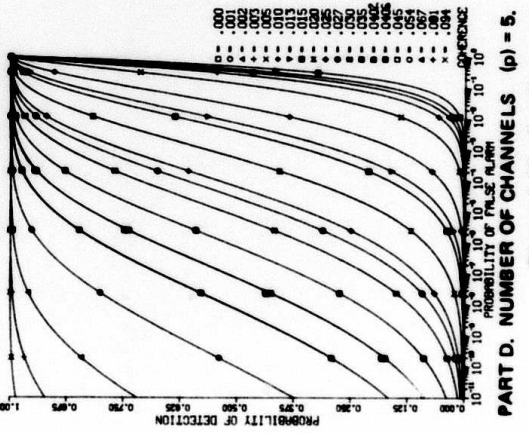
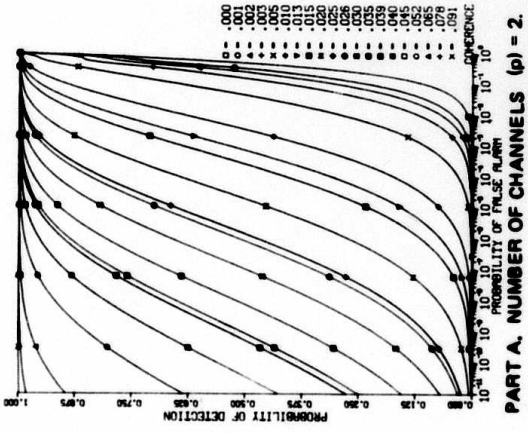
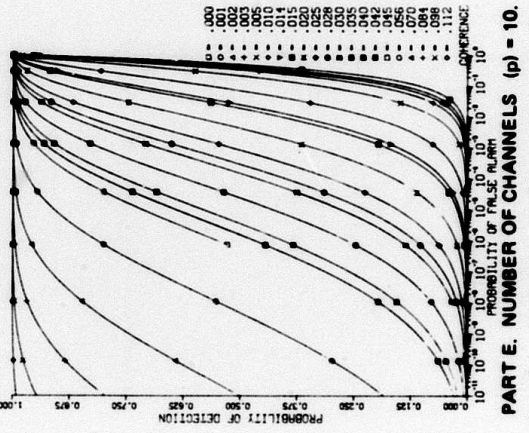
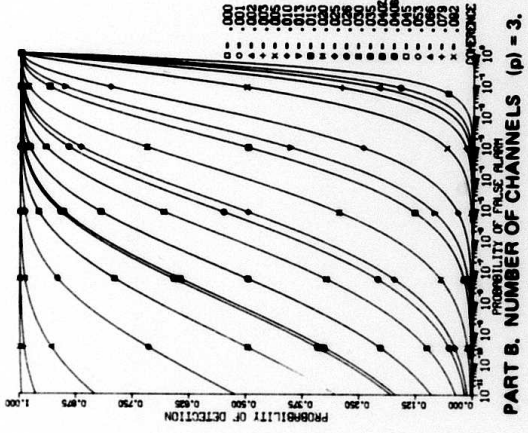
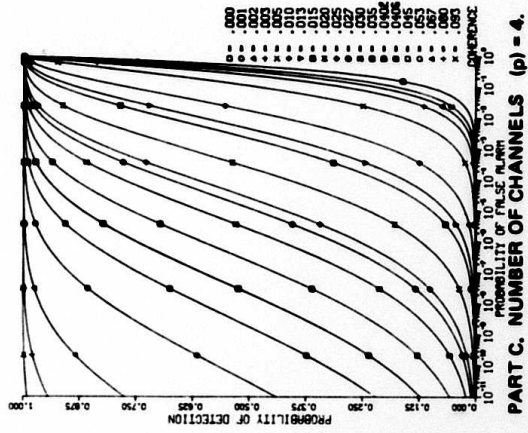
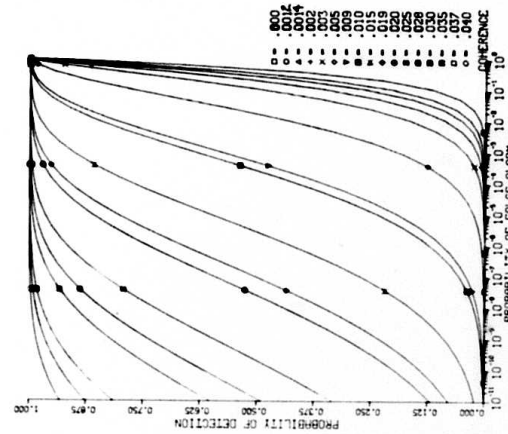
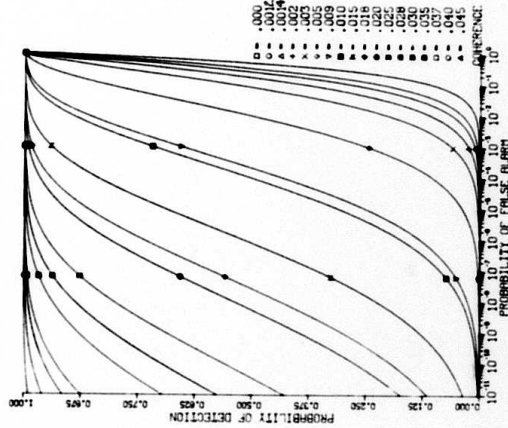


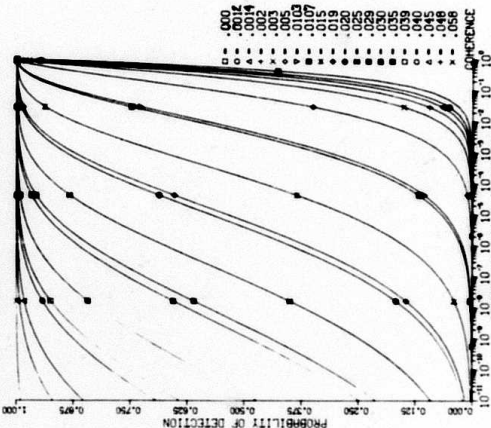
Figure 6.23. Semilog receiver operating characteristics: performance curves for the multiple-coherence test statistic. Number of degrees of freedom (N) = 512.



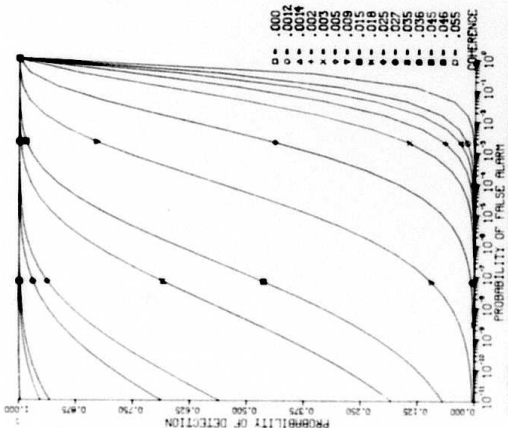
PART C. NUMBER OF CHANNELS (p) = 4.



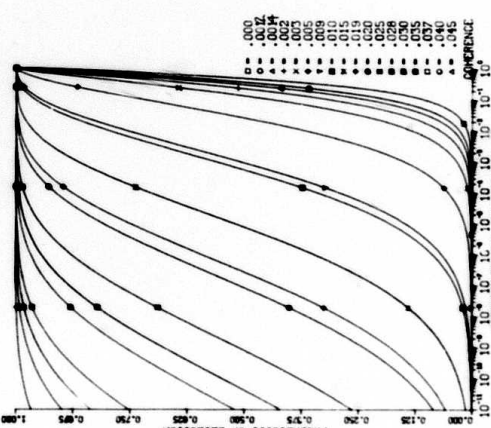
PART B. NUMBER OF CHANNELS (p) = 3.



PART E. NUMBER OF CHANNELS (p) = 10.



PART A. NUMBER OF CHANNELS (p) = 2.



PART D. NUMBER OF CHANNELS (p) = 5.

Figure 6.24. Semilog receiver operating characteristics: performance curves for the multiple-coherence test statistic. Number of degrees of freedom (N) = 1024.

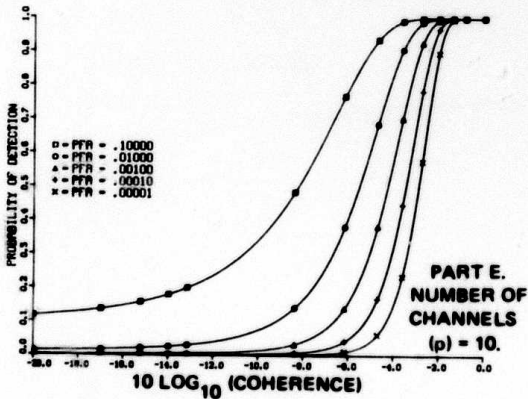
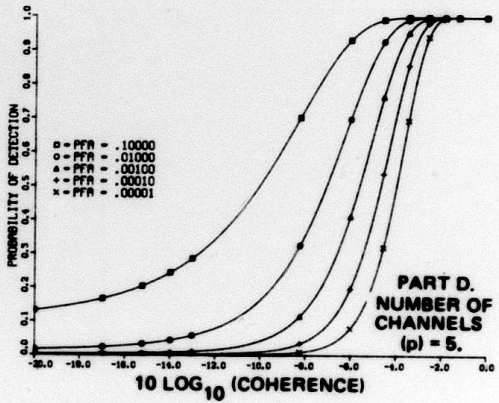
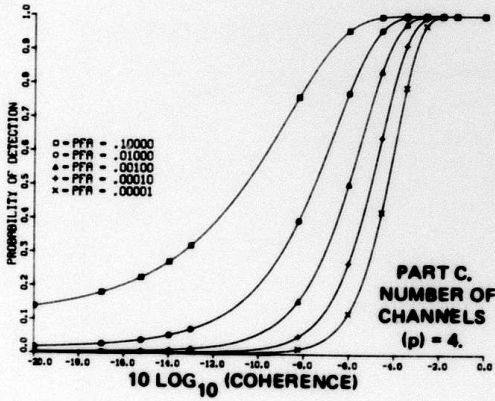
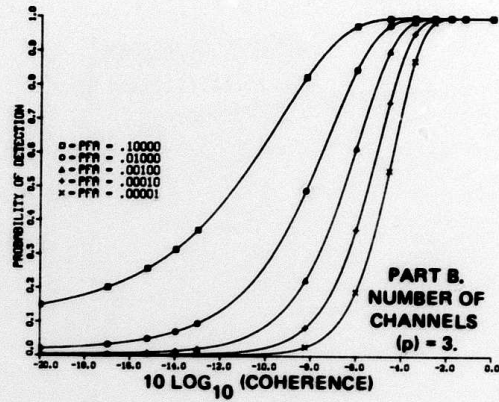
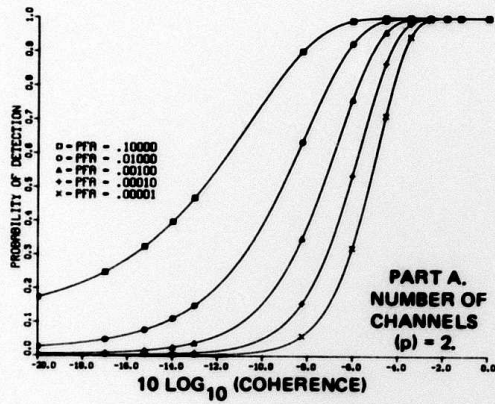


Figure 6.25. Probability of detection as a function of $10 \log_{10}$ (true coherence) for the multiple-coherence test statistic. Number of degrees of freedom (N) = 32.

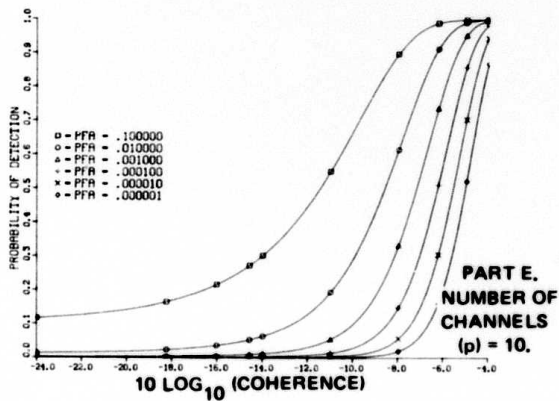
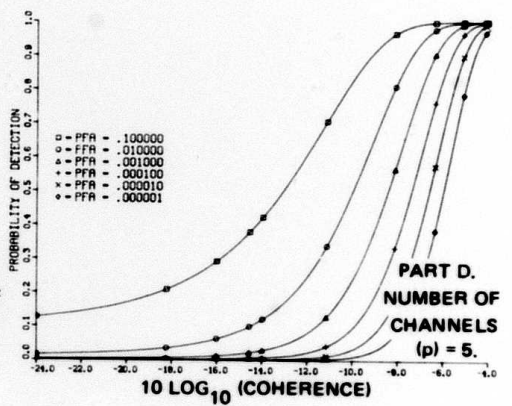
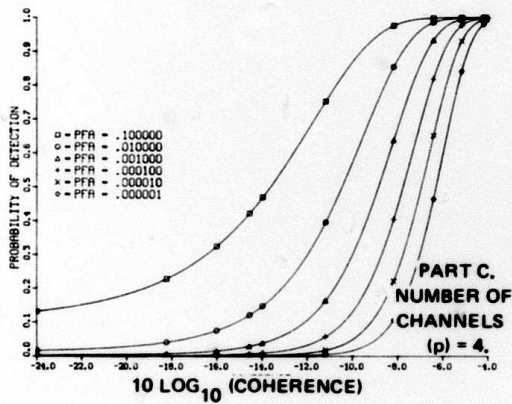
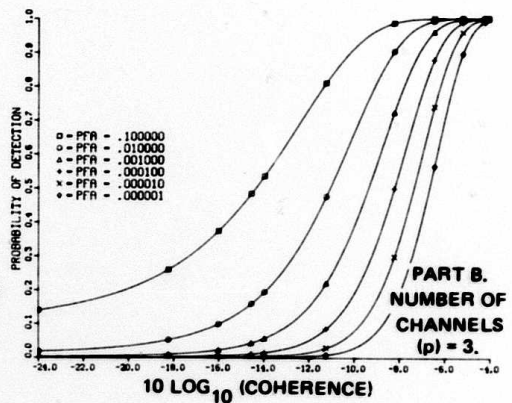
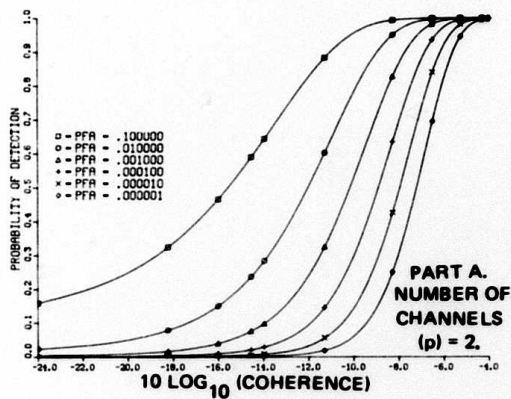


Figure 6.26. Probability of detection as a function of $10 \log_{10}$ (true coherence) for the multiple-coherence test statistic. Number of degrees of freedom (N) = 64.

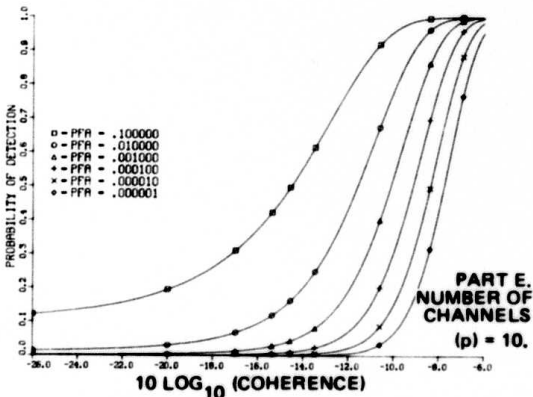
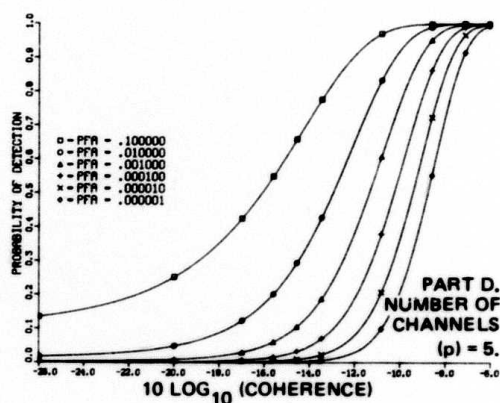
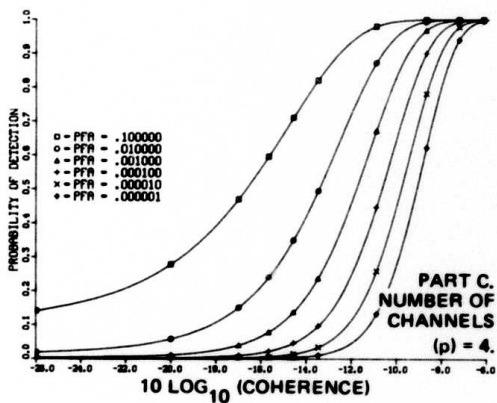
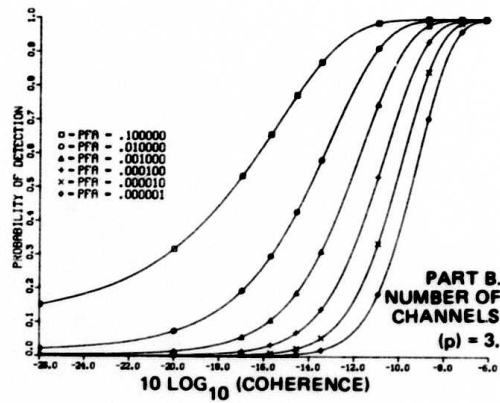
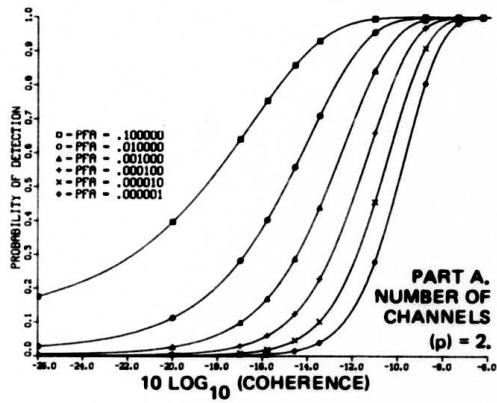


Figure 6.27. Probability of detection as a function of $10 \log_{10}$ (true coherence) for the multiple-coherence test statistic. Number of degrees of freedom (N) = 128.

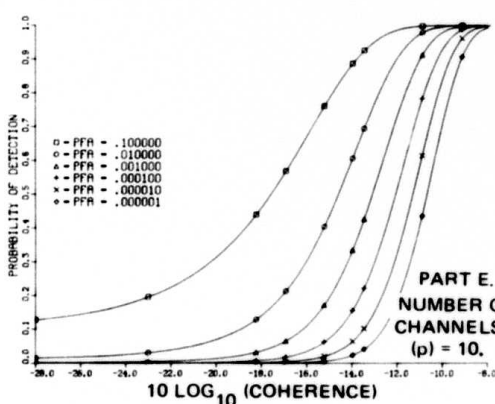
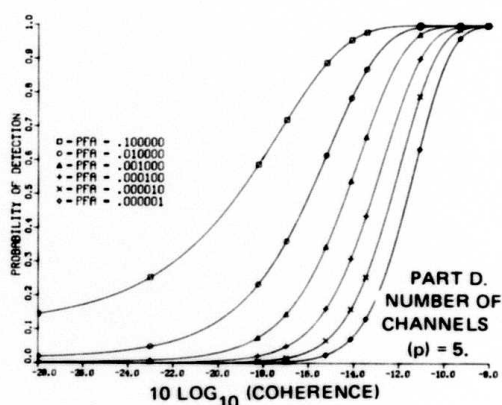
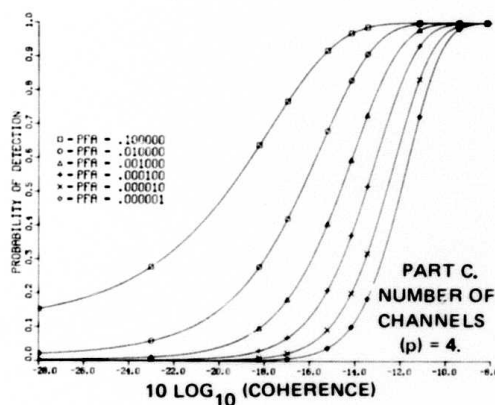
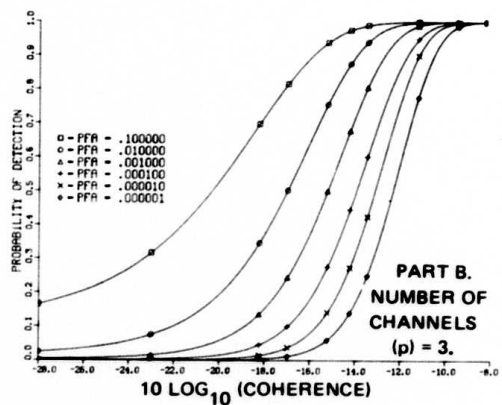
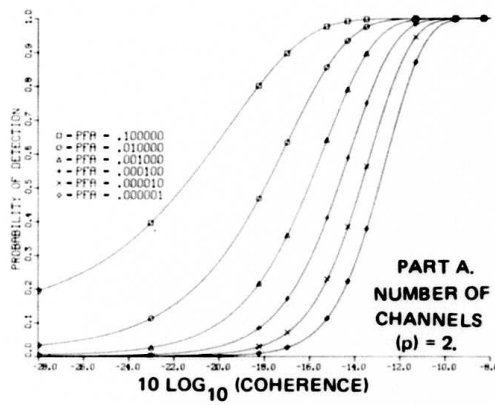


Figure 6.28. Probability of detection as a function of $10 \log_{10}$ (true coherence) for the multiple-coherence test statistic. Number of degrees of freedom (N) = 256.

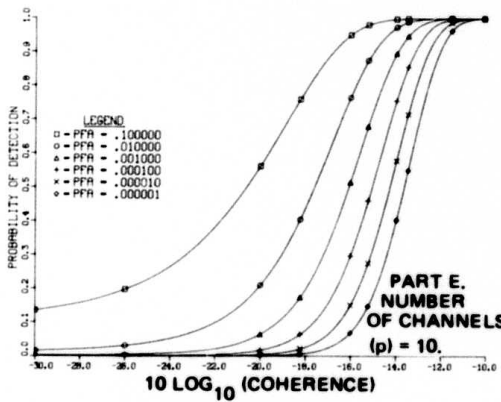
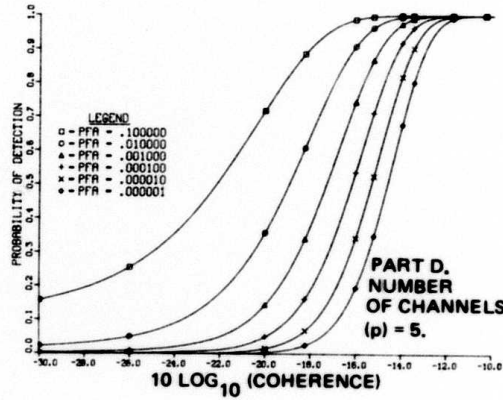
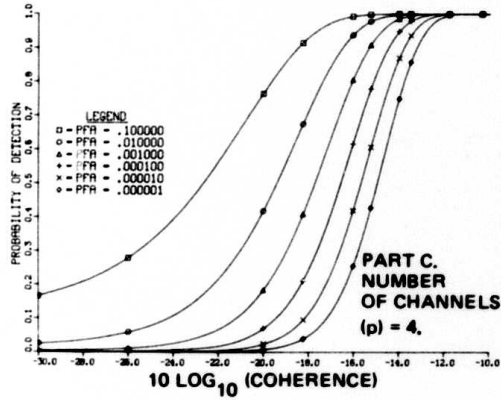
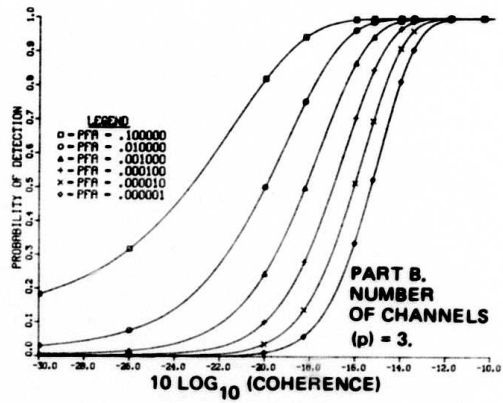
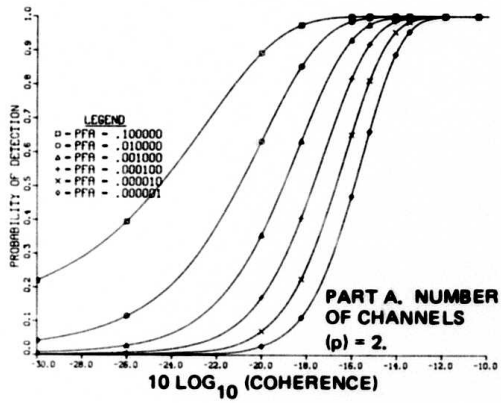
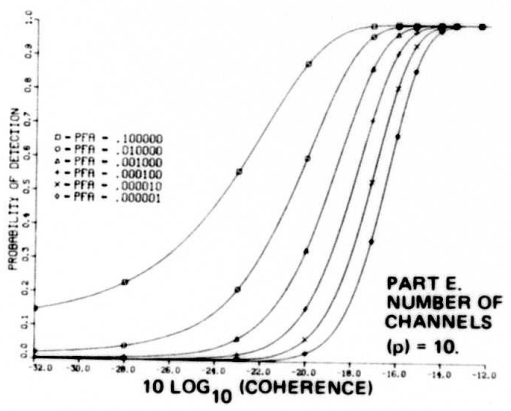
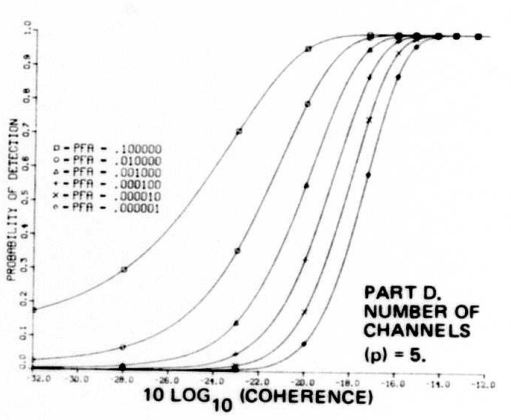
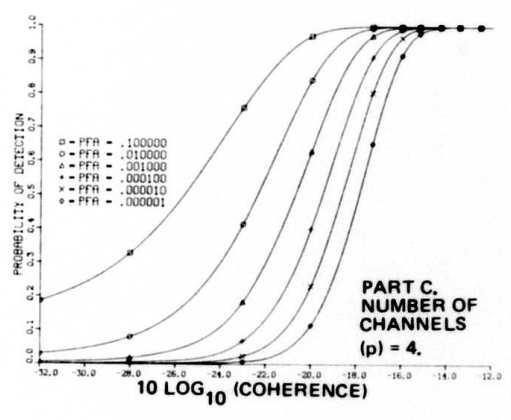
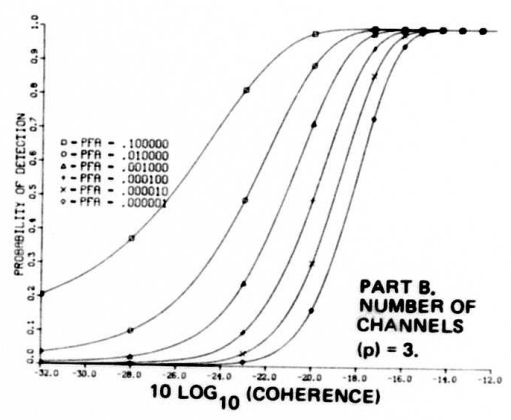
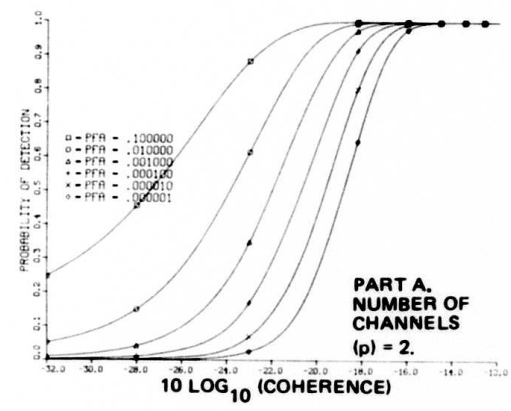


Figure 6.29. Probability of detection as a function of $10 \log_{10}$ (true coherence) for the multiple-coherence test statistic. Number of degrees of freedom (N) = 512.



(U) Figure 6.30. Probability of detection as a function of $10 \log_{10}$ (true coherence) for the multiple-coherence test statistic. Number of degrees of freedom (N) = 1024.

SECTION 7.0 REFERENCES

1. Munk, W. H., Snodgras, F. E., and Tucker, M. J., Spectra of Low-Frequency Ocean Waves, Bulletin, Scripps Institution of Oceanography, Volume 7 (1959), pgs. 283-361.
2. Cox, Henry, "Coherence in Multiple Random Processes," paper presented at Sixty-Ninth Meeting of the Acoustical Society of America, Washington, D.C., 2-5 June 1965.
3. Jenkins, G. M., and Watts, D. G., Spectral Analysis, Holden Day, California, 1968.
4. Rosenblatt, M. (Ed.), Symposium on Time Series Analysis, John Wiley and Sons, New York, 1963.
5. Bendat, J. S., and Piersol, A. G., Random Data, Analysis and Measurement Procedures, Wiley-Interscience, New York, 1971.
6. Enochson, D. L., and Otnes, R. K., Programming and Analysis for Digital Times Series Data, The Shock and Vibration Information Center, United States Department of Defense, 1968.
7. Goodman, N. R., "Statistical Analysis Based on a Certain Multivariate Complex Gaussian Distribution (An Introduction)," Annals of Mathematical Statistics, Vol. 34, No. 1, pp. 152-177, March 1963.
8. Carter, C. G., Estimation of the Magnitude-Squared Coherence Functions, Naval Underwater Systems Center Technical Report 4343, 1972.
9. Goodman, N. R., "Measurement of Matrix Frequency Response Functions and Multiple Coherence Functions," Measurement Analysis Corporation Technical Report AFFDL-TR-65-66, June 1965.
10. Gradshteyn, I., and Ryzkik, I., Table of Integrals, Series and Products, Academic Press, New York, 1965.
11. Abramowitz, M., and Slegun, A., Handbook of Mathematical Functions, Dover Publications, New York, 1970.
12. Szego, G., "Orthogonal Polynomials," American Mathematical Society Colloquium Publication No. 23, 1959.

13. Van Trees, H. L., Detection, Estimation and Modulation Theory Part I, John Wiley and Sons, 1967.
14. Helstrom, C., Statistical Theory of Signal Detection, Pergamon Press, 1968.
15. Whalen, A. D., Detection of Signals in Noise, Academic Press, 1971.